Psychological Review
2013, Vol. 120, No. 1, 230–254

0033-295X/13/$12.00 DOI: 10.1037/a0030970

Critical Branching Neural Networks

Christopher T. Kello
University of California, Merced

It is now well-established that intrinsic variations in human neural and behavioral activity tend to exhibit scaling laws in their fluctuations and distributions. The meaning of these scaling laws is an ongoing matter of debate between isolable causes versus pervasive causes. A spiking neural network model is presented that self-tunes to critical branching and, in doing so, simulates observed scaling laws as pervasive to neural and behavioral activity. These scaling laws are related to neural and cognitive functions, in that critical branching is shown to yield spiking activity with maximal memory and encoding capacities when analyzed using reservoir computing techniques. The model is also shown to account for findings of pervasive 1/f scaling in speech and cued response behaviors that are difficult to explain by isolable causes. Issues and questions raised by the model and its results are discussed from the perspectives of physics, neuroscience, computer and information sciences, and psychological and cognitive sciences.

Keywords: criticality, power law, 1/f noise, neuronal avalanche, fractal spike train

Variability is the essence of neural and behavioral activity, and variability is what theories of cognition must ultimately account for. Most theories of neural and behavioral activity focus on explaining how variations are either caused by experimental manipulations, or coincident with external variations. This is not surprising, given that observing how systems are affected by external factors is a universal method of scientific inquiry. However, if one focuses on external factors exclusively, then much of the story is left untold. Oftentimes, scientists can ascribe only small amounts of neural and behavioral variation to experimental manipulations and correlational factors.

In many neural and behavioral experiments, the lion's share of variability in measurements appears to be intrinsic to the biological and cognitive systems being measured. Energy and matter constantly flow through all biological systems, including nervous systems (i.e., they are open, non-equilibrium thermodynamic systems; Hotton & Yoshimi, 2011; Katchalsky & Kedemo, 1962; Swenson & Turvey, 1991). This flow produces variations best ascribed to the structures and processes comprising the systems being measured. Studying the nature of these *intrinsic variations* is a complementary method of scientific inquiry that is also universal, yet not pursued as much as external factors in neural and behavioral studies. One reason is that researchers often view intrinsic variations as uninformative with regard to functions like perception, attention, memory, and language. However, recent data and theory suggest otherwise.

Intrinsic variations are defined empirically as variations observed when experimental manipulations are minimized, for example, when spontaneous neural activity is measured in cortical slice preparations (Beggs & Plenz, 2003), or in brain images during the wakeful resting state (Raichle & Gusnard, 2005), or when behavioral acts are repeated with minimal variation in intentions and measurement conditions (Beltz & Kello, 2006). If one assumes that intrinsic variations are the sum of many unknown effects that are largely independent of each other, then whatever the nature of those individual effects might be, their sum will often tend toward "white noise," that is, random samples drawn from a normal distribution (for an exception, see Granger, 1980; Granger & Joyeux, 1980). Results, however, do not bear out this assumption.

In many different studies of neural and behavioral activity, intrinsic variations have been reported to resemble *scaling laws* across a wide range of scales (Kello et al., 2010), which are decidedly unlike white noise. Some are power law tails in distributions of measured values, such as reaction times (Holden, Van Orden, & Turvey, 2009) and bursts of neural activity (Poil, van Ooyen, & Linkenkaer-Hansen, 2008). Others are long-range temporal correlations in measured time series, that is, 1/f scaling, also known as 1/f noise. 1/f fluctuations have been found in estimates of length and duration intervals (Gilden, Thornton, & Mallon, 1995), for instance, and in electro- and magnetoencephalogram spectra (EEG and MEG; Linkenkaer-Hansen, Nikouline, Palva, & Ilmoniemi, 2001). These findings add to a vast literature on scaling laws found throughout nature, but their general meaning is an ongoing matter of debate (Gilden, 2001; Van Orden, Holden, & Turvey, 2003; Wagenmakers, Farrell, & Ratcliff, 2004).

The views and conclusions contained herein are those of the author and should not be interpreted as representing the official policies, either expressly or implied, of the Defense Advanced Research Projects Agency (DARPA) or the U.S. Government. This research was supported by awards from the National Academies Keck Futures Initiative, the National Science Foundation (Grants BCS 0842784 and 1031903), and DARPA under Contract HR0011-09-C-0002. I thank John Beggs, Rick Dale, Marty Mayberry, David Noelle, Guy Van Orden, Michael Spivey, and members of the Cognitive Mechanics Lab (University of California, Merced) for comments and discussions.

Correspondence concerning this article should be addressed to Christopher T. Kello, Cognitive and Information Sciences, School of Social Sciences, Humanities, and Arts, University of California, Merced, 5200 North Lake Road, Merced, CA 95343. E-mail: ckello@ucmerced.edu

Currently, no theory is widely accepted to explain scaling laws in variations intrinsic to neural and behavioral activity, although explanations have been offered for each given result. The more general debate is between explanations that consider widespread scaling laws as coincidences due to multifarious origins, versus explanations that consider scaling laws as expressions of general principles of cognitive function at both neural and behavioral levels of analysis. The same basic debate between domain-specific versus domain-general explanations of scaling laws has been unfolding throughout the sciences for decades, suggestive of a deep issue at stake.

If scaling laws are expressions of general principles, then those principles may illuminate relations between neural and behavioral scales of analysis. Relating these scales is a central issue in the psychological and cognitive sciences, and connectionist theories are perhaps the most explicit and formal in addressing this issue to date. Connectionist models use networks of neuron-like processing units to account for behavioral data using neural-like mechanisms of learning, memory, and representation. Thus, neural principles and mechanisms are explicitly related to behavioral phenomena, but models are mostly silent with regard to intrinsic variations. The reason can be traced back to a point made earlier—most theories of cognition are empirically evaluated in terms of their ability to explain and predict variations caused by external factors. For instance, many connectionist models aim to simulate the effects of stimulus or task manipulations on reaction times or response errors. These manipulations cause extrinsic variations in behavior and, by extension, in the underlying cognitive processes.

Connectionist models are designed to produce extrinsic variations in response to changing inputs and feedback (stimuli and task conditions, respectively). Simulations are typically aimed at aggregate data in which individual variations have been averaged away. This level of theorizing is the foundation of connectionist modeling, and the behavioral and cognitive sciences in general, but it comes with an implicit disregard for intrinsic variations. This disregard has a consequence that is made clear by asking, what do models do when inputs and error signals are held constant, that is, when a model's intrinsic variations are expressed? Either immediately or after a few simulation cycles, standard feed-forward networks with sigmoidal or similar units will produce no variations at all, because unit inputs and outputs are driven entirely by external factors. A learning mechanism like back-propagation may introduce some initial, transient variations until error is minimized, but these variations would carry no theoretical weight. One could impose "intrinsic" variability by injecting noise, but this would be hollow without a noise mechanism and theoretical motivation for it.

Recurrent and oscillatory networks have a more meaningful capacity for intrinsic variations that settle on point or limit cycle attractors (Cao & Wang, 2000; Ermentrout, 2001; Large & Kolen, 1994; Spivey, 2007). These models are either constrained to produce point or limit cycle attractors (e.g., Carpenter & Grossberg, 1987; Hopfield, 1982), or shaped by learning mechanisms to produce them (e.g., Harm & Seidenberg, 1999; Hinton, 1989). Attractors have proven powerful for simulating behavioral data and theorizing cognitive processes, but they are ill-equipped to handle intrinsic variations. The problem is that when extrinsic sources of variability are held constant, point attractors produce no variations and limit cycles produce only regular variations. By contrast, biological and cognitive systems produce highly irregular variations when extrinsic factors are minimized, sometimes as fluctuations around more regular variations (e.g., variations in EEG waves).

A smaller number of connectionist models have been designed to produce more sustained, complex variations in the form of learned trajectories through activation space, as in certain kinds of simple recurrent networks (Elman, 1990) and continuous-time recurrent networks (Pearlmutter, 1995). However, even for these models, the emphasis is on variations in extrinsic factors and how they cause variations in the learning and production of trajectories. The capacity for intrinsic variation is left unexamined. Boltzmann machines and related generative models provide an interesting counterpoint to the above examples (Ackley, Hinton, & Sejnowski, 1985; Hinton, Osindero, & Teh, 2006), because stochastic, intrinsic variability is essential for learning and modeling distributions over inputs and features. However, these stochastic variations typically are not intended to simulate neural or behavioral variations.

In the present study, a spiking neural network model is developed to simulate the complex, irregular variations that manifest as scaling laws in measures of intrinsic neural and behavioral activity. The model relates these scaling laws to computational capacity and, in doing so, provides a bridge for modeling cognitive performances. There are three main features and principles of the model to highlight up front:

- *Spike dynamics*. Connectionist models mostly use continuous activation functions, mainly because they are differentiable. Instead of continuous activations, the present model uses discrete events on neuron-like units at instantaneous points in time. Discrete events are used mainly because they can be counted and because tracking numbers of events is essential to theorizing dynamics as a *branching process* (Harris, 1989). Also, neural network activity can be modeled using discrete events corresponding to postsynaptic potentials (PSPs) and action potentials (spikes). A PSP may be followed by a spike, which may trigger further PSPs and spikes. In the present model, these events are simulated asynchronously with arbitrary precision in time (i.e., event-based processing; Mattia & Del Giudice, 2000).
- *Critical branching*. In theorizing spike dynamics as a branching process, each spike may be "blamed" for branching into one or more subsequent spikes. The *branching ratio* of a network is the expected number of branches per spike, and a one-to-one ratio is known as *critical branching* (Zapperi, Lauritsen, & Stanley, 1995). The critical branching point is an attractor of the present model by virtue of a simple, local mechanism that enables and disables connections among units. Critical branching regulates spike propagation, and spike dynamics exhibit scaling laws by virtue of attraction to a critical point (Beggs & Plenz, 2003; Haldeman & Beggs, 2005).
- *Reservoir computing*. Critical branching spike dynamics are shown to support a generic capacity for computation that does not rely on learning per se. The idea of using the generic capacity of dynamics for computation goes by the name of *reservoir computing* and has been studied extensively in recent years (Jaeger, Maass, & Principe, 2007; Maass, Natschlager, & Markram, 2002). Reservoir computing techniques are used herein to assess the computational capacities of self-tuned networks and show one way

that critical branching networks may support neural and cognitive functions.

The study begins with a review of empirical work on intrinsic variations, first in neural activity and then behavioral activity. *Critical phenomena* are then introduced as theoretical background, followed by a formal description of the critical branching neural network model. Three sets of simulations are reported that account for scaling law observations across multiple measures of neural and behavioral activity, including the pervasiveness of 1/f scaling in human behavior (Kello, Anderson, Holden, & Van Orden, 2008; Kello, Beltz, Holden, & Van Orden, 2007). Scaling laws are simulated by virtue of the critical branching mechanism that is formulated, which also results in maximal memory and encoding capacities of spike dynamics. The study ends with a discussion of issues and questions raised by the model, from the perspectives of physics, neuroscience, computer and information sciences, and psychological and cognitive sciences.

The Character and Meaning of Intrinsic Variations

The study of intrinsic variations has been underway in neuroscience for many years. One reason why neuroscientists have paid attention to intrinsic variations is simply because neurons and neural systems tend to exhibit ongoing, spontaneous spiking activity. This is true *in vitro* as well as *in vivo*, and it is true for single-cell recordings (Stein, Gossen, & Jones, 2005), local field potentials (LFPs; Arieli, Sterkin, Grinvald, & Aertsen, 1996), EEGs (Laufs et al., 2003), MEGs (Z. Liu, Fukunaga, de Zwart, & Duyn, 2010), and brain imaging (Raichle et al., 2001).

These measures of intrinsic neural activity are different in many respects. As examples, single-cell recordings measure individual spikes, LFPs measure extracellular changes in voltage due to PSPs occurring within millimeters of an electrode, EEGs measure summed PSPs of many thousands or millions of aligned neurons near the scalp, and functional magnetic resonance imaging (fMRI) measures correlates of hemodynamics. The neural mechanisms responsible for variations observed in each of these measures are complex and multifaceted, and their differences give rise to different kinds of variations.

However, with due respect to differences, scaling laws stand out as a common finding throughout these measures of neural activity. In single-cell recordings, a number of scaling laws have been found in the variability of spike times, including interspike intervals (ISIs; Baddeley et al., 1997), the coefficient of variation (Usher, Stemmler, Koch, & Olami, 1994), and the temporal clustering of spikes (Teich, Heneghan, Lowen, Ozaki, & Kaplan, 1997). In LFP, EEG, and MEG recordings, measurements of bursting in activity have been found to be distributed in power laws known as "neuronal avalanches" (for a recent review, see Hahn et al., 2010), where the probability of observing a burst of size S goes as $P(S) \sim 1/S^{\alpha}$, where $\alpha \sim 3/2$. Temporal fluctuations at all levels have been found to resemble 1/f scaling laws (see Bédard & Destexhe, 2009), where spectral power is related to frequency as $S(f) \sim 1/f^{\alpha}$, with $\alpha \sim 1$. Measurement conditions in these studies elicited intrinsic variations, because they were mostly devoid of experimental manipulations across measurements. For *in vitro* recordings (Beggs & Plenz, 2003), cortical slices are prepared to elicit spontaneous bursts of activity. In single-cell recordings from awake animals (Hahn et al., 2010), stimuli are neutral and unvaried. In recordings of human brain activity (Poil et al., 2008), participants are instructed to simply hold still with their eyes closed.

The study of intrinsic variations is not as well developed in behavioral activity as it is for neural activity. One reason is that it is unclear how to elicit intrinsic variations in behavior, because behavioral activity is not spontaneous in the same way that neural activity is. Kello and colleagues (Kello et al., 2008, 2007) have endeavored to define the conditions for measuring intrinsic variations so they apply to both neural and behavioral activity. In particular, intrinsic variations are elicited most clearly when minimizing external perturbations, manipulations, and contingencies in measurements. One way to satisfy these conditions in behavior is to instruct participants to minimize all movements, as is done when participants stand still and measurements are taken of unavoidable sways in posture (Riley & Turvey, 2002). While postural sway has been used as an index of cognitive activity (Shockley, Santana, & Fowler, 2003), minimization of movements is generally limited as a measurement protocol for studying cognitive functions. A broader way to elicit intrinsic variations is to consider that repetitive behaviors also minimize external factors, specifically with respect to measurements taken equivalently across repetitions. Thus, intrinsic variations can be elicited in any repeated behavior and measured more clearly as repetitions are executed more consistently from one to the next.

Ironically, repeated measures are commonly used to elicit subtle extrinsic variations in relatively small changes to stimuli or responses across repetitions. For instance, repeated responses to words or pictures are widely used in many areas of experimental psychology, and at the level of stimulus or response category, conditions do not change across trials. Subtle, within-category changes appear to create only small extrinsic variations (typically far less than half the variance), and variations due to measurement error are also demonstrably small (e.g., Gilden, 2009; Kello & Kawamoto, 1998). Thus, the largest portion of variance under these conditions is intrinsic by this definition. This portion grows even larger when stimulus and response conditions are held as constant as possible across trials, for example, by repeating the same particular movement or same particular utterance over and over again.

Intrinsic variations in behavior have been examined in all the conditions just reviewed, and as with neural activity, scaling laws appear widespread in distributional and temporal measures of behavioral activity. For instance, postural sway exhibits 1/f scaling (Duarte & Zatsiorsky, 2001), and pole balancing exhibits power law distributions in the amplitudes of excursions from the center point (Cluff & Balasubramaniam, 2009). In more cognitive performances, reaction times to words have been found to be well modeled by mixtures of lognormal and power law distributions (Holden et al., 2009), and fluctuations in naming latencies and lexical decision times have both been found to follow 1/f scaling laws (Van Orden et al., 2003). Fluctuations follow 1/f scaling laws even more closely when behaviors are even more repetitive, for example, when the same time or distance interval is estimated repeatedly (Gilden et al., 1995) or when acoustic measures are taken of the same word spoken repeatedly (Kello et al., 2008).

None of these data sets follow scaling laws perfectly, but they comprise a body of findings that calls for explanation. Why do

measures of intrinsic variations so often resemble scaling laws, and why are those laws more closely followed when conditions are better suited to measuring intrinsic variations? Some researchers who examine scaling laws nonetheless put this question aside, because they are more interested in formulating domain-specific explanations. For instance, oscillatory timing models applied to bimanual finger tapping have been modified to produce 1/f scaling in their fluctuations (Torre & Wagenmakers, 2009), but the general association between scaling laws and intrinsic variations in neural and behavioral activity falls outside the purview of such domain-specific models.

It has been argued that scaling laws are generally associated with intrinsic variations because scaling laws are *pervasive* to interactions among components of biological and cognitive systems (Kello et al., 2007). Pervasiveness in this sense is based on two premises. First, all measures of biological and cognitive systems reflect interactions among components at some scale of analysis, be they molecules, neurons, organs, organisms, or groupings of organisms (Simon, 1973). Second, all measures of intrinsic variations reflect the general character of these interactions under a relatively constant flow of matter and energy, due to the minimization of extrinsic variations. Given these premises, the word "pervasive" is used to denote the hypothesis that scaling laws are not restricted or isolated to particular components of these systems. Instead, all component interactions may exhibit scaling laws under conditions of intrinsic variation, hence their hypothesized pervasiveness.

Domain-specific hypotheses and the pervasive hypothesis are at two different levels of analysis, and so do not compete directly. However, domain-specific hypotheses often assume that scaling laws originate from specific components and are therefore isolable to those components. This broader hypothesis of isolability is at the same level as pervasiveness, and these two hypotheses make competing predictions that have been tested in two previous studies. First, Kello et al. (2007) found that intrinsic fluctuations in simple and choice key-press response times were uncorrelated with those in the very same key-press durations, yet both exhibited 1/f scaling. Parallel yet uncorrelated streams of 1/f fluctuations are accommodated by the pervasive hypothesis, provided that measures reflect distinct degrees of freedom in movement. The isolable hypothesis must posit an independent scaling law component for each mutually independent stream of 1/f fluctuations—two in this case.

Kello et al. (2008) argued that such isolable components would be difficult to posit given the pattern of results, and a subsequent study provided an even stronger test of the isolable hypothesis. Many mutually independent streams of intrinsic variation were elicited in the repetitions of a spoken word ("bucket"), and all acoustic measurement series exhibited 1/f scaling. The exact number of independent streams is difficult to determine, but Kello et al. estimated about 30 linearly separable streams using principal components analysis. In a subsequent reanalysis, Moscoso del Prado Martín (2011) applied information theoretic analyses to the data and estimated about 12 mutually independent streams. By either count, the isolable hypothesis requires a painfully ad hoc proliferation of separate scaling law components, whereas the pervasive hypothesis accommodates the results naturally: There are many degrees of freedom in the speech articulators that are reflected in speech acoustics, and each has the capacity to exhibit distinct intrinsic variations (Kello, 2011).

Pervasive Scaling Laws and Criticality

Based on results discussed thus far, let us accept for now that scaling laws of various kinds are widely associated with intrinsic variations in neural and behavioral activity and are pervasive to them. If intrinsic variations always reflect inherent component interactions, then what kind of interactions would lead to pervasive scaling laws? Physics provides us with a ready answer in *critical phenomena* studied in statistical mechanics (Sornette, 2004; Stanley, 1987).

The field of statistical mechanics describes how the macroscopic quantities of systems arise statistically from their microscopic components and interactions among them. For some simple systems, interactions can be disregarded because macroscopic quantities are simple aggregates of component quantities, such as heat being an aggregate of particle energies in a gas. In more complex systems, however, microscopic interactions play an essential role in macroscopic behavior, as in Rayleigh–Benárd patterns of convection currents created by heat flow in liquids under certain thermodynamic conditions. Specifically, *critical points* are formal conditions under which macroscopic quantities may be significantly affected by microscopic interactions. Criticality has provided scientists of all kinds with a means of modeling organized patterns observed in nature, whose origins would otherwise have no explanation. These patterns include pervasive scaling laws.

So what kinds of interactions will yield critical points and associated scaling laws? A comprehensive treatment of this question is beyond the present scope (for reviews, see Bak & Paczuski, 1995; Jensen, 1998), but for the present purposes, critical points occur when interactions are poised to take a system toward multiple possible macroscopic states (i.e., poised near a second-order phase transition). Many illustrative examples can be drawn from across the sciences, perhaps the most famous being the Ising model of ferromagnetism (see Kello & Van Orden, 2009). A more pertinent illustration can be drawn from the interactions among spiking neurons, particularly with respect to excitatory versus inhibitory effects.

Signaling among neurons can be expressed in terms of three types of voltages—membrane potentials, PSPs, and action potentials. When the membrane potential of a given neuron exceeds threshold, an action potential triggers PSPs over its axonal synapses. PSPs from excitatory neurons increase the membrane potentials of postsynaptic neurons, whereas PSPs from inhibitory neurons decrease them. There also may be tonic effects on voltages due to leakage and ambient concentrations of neurotransmitters, for instance. In terms of statistical mechanics, neurons and synapses are the microscopic components, and neuron interactions are expressed as the interplay of excitatory and inhibitory voltage signals among those components. The macroscopic variable of interest is the net potential V_{net}, and the network may head toward two different macroscopic states depending on the long-term expected value of its derivative, dV_{net}/dt. If $dV_{net}/dt > 0$ on average, then spike rate grows to a maximum that depends on refractory periods and membrane resistances. If $dV_{net}/dt < 0$, then spike rate diminishes to zero.

Maximal and minimal spike rates are two possible macroscopic states of spiking neural networks. Like ideal gases, the interactions among neurons can be disregarded when networks converge toward one of these two states. In order for neural networks to behave differently from gases, they must stay near $dV_{net}/dt = 0$, where V_{net} is a moderate level of excitiation. When $dV_{net}/dt \sim 0$, microscopic interactions may have effects on macroscopic patterns of spiking over neurons. A mean excitatory voltage is maintained between neurons and their extracellular environments, and a balance is struck between excitatory and inhibitory effects on membrane potentials. Balancing excitation and inhibition is a well-known concept studied in slice preparations of neural tissue (Higley & Contreras, 2006; Shew, Yang, Petermann, Roy, & Plenz, 2009; Shu, Hasenstaub, & McCormick, 2003) as well as computational models of neural networks (Brunel, 2000; van Vreeswijk & Sompolinsky, 1996), although this balance is not always examined as a critical point. Excitatory and inhibitory effects can be carefully balanced by the modeler, or homeostatic mechanisms can be formulated to regulate this balance. If formulated as a critical point, then spiking activity is theorized to exhibit critical phenomena (Shin & Kim, 2006; Usher, Stemmler, & Olami, 1995), including scaling laws.

Computational Capacity and Critical Branching

A spiking model that maintains $dV_{net}/dt \sim 0$, and in doing so exhibits pervasive scaling laws in neural and behavioral activity, would simulate a wide range of empirical results heretofore not captured by one model. However, behavioral and cognitive scientists might question the relevance of such a model to theories of cognitive function. The model would be relevant to neural function because, without this balance, spikes would become either useless or unavailable for coding information. However, from a functionalist point of view, balancing excitation and inhibition may only provide the physical basis for cognitive function, without directly informing theories of cognition.

The alternative point of view is that, as a critical point, this balance confers computational properties that are adaptive and relevant to cognitive functions. This alternative has its roots in work on cellular automata showing that, with an appropriate set of update rules, the inherent dynamics at critical points between order-disorder transitions have a generic capacity for transmission, storage, and modification of information (Crutchfield & Young, 1990; Langton, 1990; Packard, 1988). Subsequent studies have further explicated this hypothesis (Mitchell, Hraber, & Crutchfield, 1999) and have developed other so-called "edge of chaos" models more akin to neural networks (Bertschinger & Natschlager, 2004; Kwok & Smith, 2005).

One way to conceptualize the relationship between criticality and cognitive function is to consider the property of *metastability* (Bressler & Kelso, 2001; Kello & Van Orden, 2009; Kelso, 1995; Rabinovich, Huerta, Varona, & Afraimovich, 2008). Recall that in near-critical systems, interactions among microscopic components may cascade across scales to have macroscopic effects. Thus, the effects of external perturbations extend forward in time and depend on the history of activity leading up the perturbations in question. That is, dynamics are context-dependent (Van Orden, Kello, & Holden, 2010). Moreover, multiplicative interactions near critical points mean that macroscopic patterns reflect conjunctions and contingencies among microscopic activities. The consequence is that metastability may support targeted, nonlinear computations based in spatially and temporally extended inputs (for an optimization example, see Kwok & Smith, 2005).

The mathematical and computational studies reviewed thus far suggest that critical points could be central to cognitive function, and also provide a comprehensive explanation of pervasive scaling laws in neural and behavioral activity. However, these studies focused on the analytic properties of models, and they formulated critical points in terms that may be difficult to relate to brain and bodily functions. By contrast, balancing excitation and inhibition is general to brain and bodily functions and may be expressed in mechanisms that are at least consistent with biological evidence. The main goal of the present study is to formulate one such mechanism and demonstrate its ability to explain pervasive scaling laws in neural and behavioral activity.

Recent work leading up to the present model began by characterizing spike dynamics as a *branching process* (Kello & Kerster, 2011; Kello, Kerster, & Johnson, 2011; Kello & Mayberry, 2010). In any given network, an ancestor spike occurring on neuron i at time t may subsequently "branch" into some number of descendant spikes at times $t + \tau_k$, where descendant spikes occur on neurons directly connected via axonal synapses, indexed by k. Thus, subsequent spikes triggered downstream do not count as descendants of neuron i, but rather as descendants of their directly connected neurons.

The expected number of descendants for each given ancestor spike is defined as the *branching ratio*, $\sigma \equiv \langle N_{post} \rangle$, where N_{post} is counted for each given ancestor spike (the denominator is implicitly one). The branching ratio of a spiking network reflects its proportion of excitation versus inhibition, taking into account other factors such as leakage and sources of voltage input to the network. This relation between branching ratio and dV_{net}/dt holds for the following reasons. If $dV_{net}/dt < 0$, then spike rates must decrease on average over time, which will cause $\sigma < 1$. If $dV_{net}/dt > 0$, then rates must increase, which will cause $\sigma > 1$. Excitatory and inhibitory effects are balanced near the critical branching ratio, $\sigma \sim 1$.

The correspondence between $\sigma \sim 1$ and a critical point at $dV_{net}/dt = 0$ is supported by analyses showing that critical points can in fact exist at critical branching (Lübeck, 2004). Critical branching dynamics have been examined in recent studies and have been found to have computational properties adaptive and relevant to cognitive function (de Arcangelis & Herrmann, 2010; Haldeman & Beggs, 2005; Kinouchi & Copelli, 2006), as they should if the corresponding critical point yields "edge of chaos" properties reviewed earlier. Moreover, critical branching processes have been shown to produce *neuronal avalanche* scaling law dynamics (Benayoun, Cowan, van Drongelen, & Wallace, 2010), as well as 1/f scaling law dynamics (Ihlen & Vereijken, 2010), as they should if critical points are generally associated with scaling laws.

These studies indicate that scaling laws and computational capacity may be associated with critical branching spike dynamics. However, they do not demonstrate pervasive scaling laws in both neural and behavioral activity, and they do not demonstrate a connection between critical branching, scaling laws, and computational capacity that can be used to model cognitive functions. Also, most of them do not explain how neural networks might

grow and maintain themselves near critical branching. de Arcangelis and colleagues (de Arcangelis & Herrmann, 2010; de Arcangelis, Perrone-Capano, & Herrmann, 2006) have addressed these aims, to some degree, with spiking network models that incorporate membrane and synaptic update rules tailored to achieve critical branching. Collectively, they found avalanche and 1/f scaling law dynamics at a neural level of analysis, although criticality may not be necessary to obtain their results. They also found neuron spike patterns to be nonlinear functions of input patterns, such as the XOR function that has similarly been used to examine the computational capacity of back-propagation in connectionist models (Rumelhart, Hinton, & Williams, 1986).

Spiking Network Model With Self-Tuned Critical Branching

The present work builds upon previous efforts to formulate a simple spiking network model. The model is simple in that it uses canonical leaky integrate-and-fire (LIF) neurons with standard synaptic weights. The canonical LIF network is extended by associating one binary state with each neuron's set of axonal synapses, and a second binary state with each individual synapse. These two binary states are switched according to simple rules that are local to each neuron and its synapses. The rules make the critical branching point an attractor of network dynamics, which has a homeostatic effect on spike activity.

One binary switch is associated with each individual synapse, such that each synapse can be in either an *enabled* or *disabled* state. Enabled synapses allow PSPs to be generated according to their synaptic strengths (as in the canonical model), while disabled synapses do not generate PSPs. Enabled and disabled states are consistent with evidence that, at least for some neurons, each synapse may switch between only two levels of strength, where one level is low enough to effectively generate no PSP (O'Connor, Wittenberg, & Wang, 2005; Petersen, Malenka, Nicoll, & Hopfield, 1998). In the present model, synapses are enabled and disabled in order to increase and decrease the estimated branching ratio σ_i local to each neuron i—the more enabled axonal synapses for a given neuron, the greater the expected branching ratio $\langle\sigma\rangle$. This relation is straightforwardly true for excitatory neurons with excitatory axonal synapses, because excitatory PSPs may trigger spikes. Although less straightforward, this relation also holds true for the enabling and disabling of *inhibitory* synapses.

To see why the enabled/disabled switch works the same for both excitatory and inhibitory synapses, the second binary switch must be introduced. The second switch is associated with each neuron's axonal tree of synapses and can be in either an *unblamed* or *blamed* state. At the time when a neuron spikes, its axonal tree of synapses is set to the *unblamed* state. That is, the spike has not yet been blamed for branching into one or more spikes. Subsequently, each time a spike occurs on the other side of one of its enabled axonal synapses, there is a chance that the axonal tree will be set to its *blamed* state. Importantly, assignment of blame does not depend on whether a neuron is excitatory or inhibitory—an excitatory neuron can be blamed directly for helping to trigger a spike, or an inhibitory neuron can be blamed indirectly for not inhibiting a spike. The critical branching mechanism uses the unblamed/blamed status of an axonal tree as a local estimate σ_i that holds during each ISI. This estimate is used probabilistically to disable synapses when $\sigma_i > 1$, and enable when $\sigma_i < 1$.

A formal description of the model centers on the *membrane potential update event* that occurs for each input j to each neuron i (see Figure 1 for equations in pseudocode format). Inputs may be PSPs from neurons projecting into neuron i via its dendritic synapses, or inputs may come from external sources. The update event starts with adding the input to the membrane potential and applying exponential decay that has occurred since neuron i's previous update event:

$$V_{i,t} \leftarrow V_{i,t'} e^{-\lambda_i (t - t')} + I_{j,t}$$

where V is the membrane potential, λ is the leak rate, t is the current time, t' is the last time that neuron i was updated, I is the input, and all variables except indices can be real-valued. This update rule is asynchronous in that each input may occur at any time t, and V is updated instantaneously, with a floor at zero. If $V > \theta_i$, a neuron-specific threshold, then an action potential (spike) is generated. At the same time, V is instantaneously reset to κ_i, a neuron-specific reset value, and neuron i is set to a refractory state for one unit time interval, during which no action potential can occur. The spike spawns a new PSP event I_k for each *enabled* axonal synapse k of neuron i, after a synapse-specific delay τ_k. The value I_k corresponds to ω_k, the weight on synapse k. $\omega_k > 0$ for excitatory neurons, and $\omega_k < 0$ for inhibitory neurons.

Each spike also triggers two local processes that comprise the critical branching self-tuning mechanism (see Figure 2). The axonal process begins by choosing one disabled axonal synapse, and the dendritic process begins by choosing one enabled dendritic synapse. There may be multiple disabled axonal synapses and

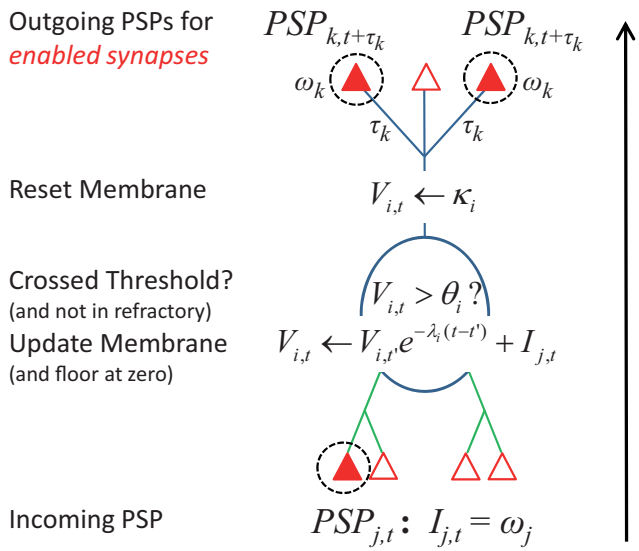

Figure 1. Pseudocode diagram for one membrane potential update, for one dendritic synapse of a neuron. In this example, the postsynaptic potential (PSP) causes the corresponding membrane potential to cross threshold, thereby triggering a membrane potential reset, along with two subsequent PSPs over two enabled axonal synapses. Operations up to the membrane reset happen instantaneously at time t but are executed in order from bottom to top. Outgoing PSPs trigger additional membrane potential updates at times $t + \tau_k$.

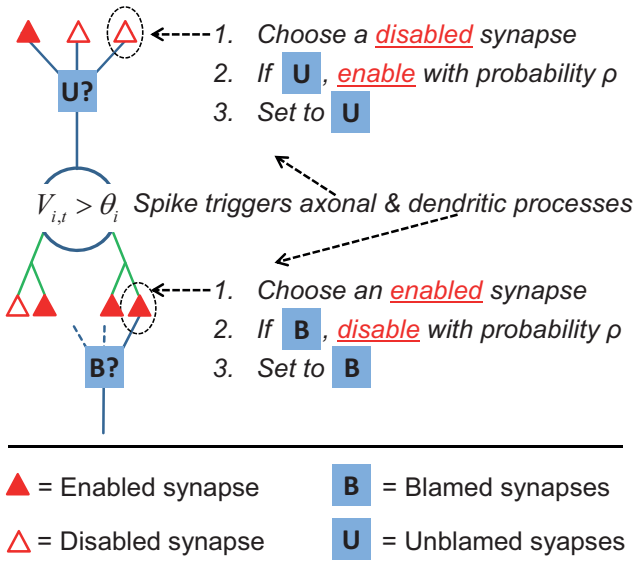

Figure 2. Pseudocode diagram of critical branching mechanism. Axonal and dendritic processes unfold independently, in orders listed. Unblamed/blamed states are switched uniformly for each set of axonal synapses.

multiple enabled dendritic synapses, but only one is chosen from each set. The choice is arbitrary with respect to the self-tuning mechanism, but for sake of clarity, suppose each synapse is chosen at random from each set (an alternate method is discussed and used below). If the chosen axonal synapse is in its unblamed state, as all synapses are initially, then the synapse is enabled with probability ρ. If the chosen dendritic synapse is in its blamed state, it is disabled with probability ρ. Finally, the axonal process ends by setting neuron *i*'s axonal synapses to their unblamed states, and the dendritic process ends by setting neuron *j*'s axonal synapses to their blamed states. Neuron *j* is the sending neuron of the chosen dendritic synapse. Note that every synapse is axonal with respect to its sending neuron and is dendritic with respect to its receiving neuron.

These local processes serve to make critical branching, $\langle\sigma\rangle = 1$, an attractor of synaptic dynamics. They do so because the unblamed/blamed switch serves to code whether a spike on neuron *i* is blamed for 0, 1, or >1 spikes during each ISI, that subsequently occur on the receiving end of its enabled axonal synapses. If neuron *i* spikes twice without receiving blame, then $\sigma_i = 0$ for that ISI. To move up toward $\sigma_i = 1$, one axonal synapse is enabled with probability ρ. By contrast, if neuron *i* receives blame more than once during an ISI, then $\sigma_i > 1$. To move down toward $\sigma_i = 1$, one axonal synapse is disabled with probability ρ, for each blame event after the first. The choice of which axonal synapse to enable or disable does not matter with respect to convergence toward critical branching, as long as $\langle\sigma\rangle$ is increased and decreased by the same amount, on average.

For the present simulations, a simple pair of choice rules was formulated to sample broadly from sets of eligible synapses and to evoke a "rich get richer" dynamic that drives some synapses to become permanently enabled. Specifically, (1) the axonal synapse *disabled for the longest time* was chosen to be enabled, and (2) the synapse *enabled for the shortest time* was chosen to be disabled. This choice was local in that longest and shortest times were relative to other axonal and dendritic synapses of a given neuron, respectively. Rule 1 ensures that the mechanism cycles through eligible synapses to be enabled, and Rule 2 creates a "backbone" of permanently enabled synapses. Some synapses are never disabled because there are always more recently enabled synapses to disable.

The creation of backbone synapses may help to minimize interference between homeostatic mechanisms like critical branching, and learning mechanisms like long-term potentiation and depression. In particular, the strengths of backbone synapses can be adjusted by learning mechanisms without being disabled by the critical branching mechanism. Note that the above choice rules require local timers to track how long each synapse has been in its current state. The timer and max/min choice mechanisms could be implemented, for example, by constant decay in the concentration of some chemical at each synapse, plus a parallel race process where the winner tends to be the synapse with the greatest or least concentration. As simple as this rule is, one might prefer an even simpler one, such as choosing at random from eligible synapses. Choosing at random had no substantive effect on results, so it is not reported here.

Critical branching is generic enough to be implemented with any kind of asynchronous spiking neuron, in any given network. The general action of the proposed mechanism is to approach critical branching by altering a network's *effective connectivity* (the set of enabled synapses) within the bounds of its *potential connectivity* (the set of all synapses). For the mechanism to work, critical branching must be attainable given potential connectivity, network parameters, and inputs. For instance, branching will remain subcritical if a network has overly weak synapses relative to its spike thresholds, or too few synapses, or too little net excitation. This is true even if all excitatory are enabled, and all inhibitory synapses are disabled.

Perhaps less obviously, branching will go supercritical if spikes introduced by external source inputs have no way to "exit" the network via "sink" neurons. Sink neurons are those whose spikes do not trigger the critical branching mechanism and, hence, are not blamed for subsequent effects on network activity. These spikes may propagate to a different network or they may simply dissipate away. Without sink neurons, a network would be effectively a closed system, like a pool with an inflow of water but no outflow. Critical branching would lead to the accumulation of spikes generated from input sources, to the point of maxing out the spike rates of neurons. Thus, the architecture of a critical branching network must support a flow of spikes from source to sink, statistically speaking.

To make this statistical flow transparent, networks were structured to have distinct groups of *source*, *reservoir*, and *sink* neurons (see Figure 3). Source neurons were excitatory and had no incoming connections. They received all inputs from sources external to the network in question and projected to reservoir neurons. All projections were random and relatively sparse, for sake of simplicity and size. Reservoir neurons were either excitatory or inhibitory, received projections from input neurons and other reservoir neurons, and projected to other reservoir and sink neurons. Sink neurons received projections from reservoir neurons and had no projections back to the network. Thus, their status as excitatory or inhibitory is irrelevant to the network in question.

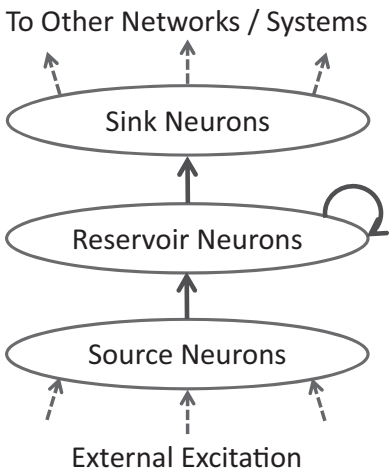

Figure 3. Architecture of critical branching networks used in Simulations 1–3. The pattern of connectivity (denoted by solid arrows) makes transparent the flow of spikes from source neurons to sink neurons via reservoir neurons. Dashed arrows denote external voltage sources (bottom) and spike dissipation (top).

This network architecture is similar in appearance to a multilayer perceptron with hidden unit recurrence, but there are important differences. Source neurons are similar to input units in standard connectionist models, but reservoir and sink neurons are *not* like hidden units and output units, respectively. Sink units do not receive targets, and reservoir units do not learn mediating representations between inputs and outputs. Rather than map inputs onto outputs, the present architecture describes a voltage source that creates a flow of spikes from source to sink via reservoir neurons. Recurrent connections allow spikes to circulate in the reservoir before leaving via the sink. Perfect critical branching corresponds to a perfectly conserved flow of spikes, in that they enter only via the source, and exit only via the sink. Subcritical branching means that spikes "leak" out of the reservoir, whereas supercritical branching means that spikes multiply as they flow through the reservoir.

Another important difference is that, in the present model, there is no mapping to learn from source to sink. The model is designed to engage homeostatic actions of the critical branching mechanism and to examine the resulting variations in spike activity (Simulation 1), the effects on computational capacity (Simulation 2), and the ability to simulate behavioral data (Simulation 3). Learning falls outside the present scope, but in Simulation 1, the compatibility of critical branching is tested with respect to a mechanism of stable Hebbian plasticity known as spike timing dependent plasticity (STDP; Dan & Poo, 2004; Markram, Lübke, Frotscher, & Sakmann, 1997). Critical branching and STDP are engaged for a common set of neurons and synapses to test whether STDP might interfere with convergence toward critical branching.

Another possible way that homeostatic and learning mechanisms may avoid interfering with each other is that they may operate on distinct sets of neurons and synapses. Critical branching networks may regulate flows of spikes into other networks whose patterns of activity are shaped by task demands. Separating the actions of these mechanisms should help minimize any possible interference between them, but the idea of homeostatic, unlearned networks is foreign to connectionist models like multi-layer perceptrons. What would be the function of networks that just regulate their flows of spikes?

One possible answer is that such networks may provide generic computational capacity for other networks to draw upon (Jaeger et al., 2007; Maass et al., 2002). The rationale is that recurrent spike dynamics are inherently nonlinear, and nonlinear dynamics are inherently difficult to adapt via learning mechanisms. Thus, nonlinear dynamics may unfold in unlearned circuits, and learned circuits may need to only implement linear transformations of unlearned, nonlinear dynamics. This approach goes by the name of *reservoir computing*, and critical branching may serve to enhance the generic capacity of unlearned, computational reservoirs (Bertschinger & Natschlager, 2004). This possible function of critical branching is tested in Simulation 2.

Finally, critical branching networks are different from connectionist networks in how they relate to neural and behavioral levels of analysis. Most generally, critical branching is based on event propagation through networks, rather than propagation of activations, error signals, or derivatives. Homeostatic regulation of event propagation is applied to spikes herein, but it may also be applied percepts, decisions, and any other kinds of neural, cognitive, and behavioral events situated in networks. The present focus on spike events and spike propagation contrasts with connectionist models based on mean-field approaches, which average over spikes and reintroduce them only as additional details, rather than essential features.

One might also assume that spike-based modeling is truer to neural mechanisms compared with mean-field approaches taken by most connectionist models. However, the present model was designed only to make fewer demands on neural mechanisms compared with propagating error signals and derivatives in connectionist models. The critical branching mechanism comprises two spike-driven processes with binary signals and switches local to each neuron and its synapses, plus extensions to axonal neighbors of dendritic synapses. Evidence for spike-driven, switch-like mechanisms is widespread (Lisman & McIntyre, 2001; McClung et al., 2004), and binary-valued synaptic strengths are simpler than those that can vary continuously over time. Also, synapses appear to have many molecular switches associated with them (Hayer & Bhalla, 2005; Micheva, Busse, Weiler, O'Rourke, & Smith, 2010), and neighboring synapses appear to communicate via glial signaling (Abraham, 2008; Stellwagen & Malenka, 2006). Thus, the proposed mechanism of switching between blamed and unblamed states is at least possible given the evidence.

Simulation 1: Critical Branching and Scaling Laws

Simulation 1 was designed to test whether (1) the model achieves critical branching under conditions of intrinsic variation, (2) critical branching spiking activity accounts for scaling laws observed at multiple levels of analysis, (3) scaling laws are maintained when STDP is included, and (4) scaling laws depend on engagement of the critical branching mechanism.

The network architecture shown in Figure 3 was used, with 40 source neurons, 1,000 reservoir neurons, and 100 sink neurons. This network size was large enough to average out idiosyncrasies of parameter initialization, yet was small enough to afford rapid

simulation and analysis. All source and sink neurons were excitatory, whereas 25% of the reservoir neurons were inhibitory. This ratio is based on the general observation that excitatory neurons outnumber inhibitory neurons by about 3 or 4 to 1 in cortex (Maass, 1997). Synaptic projections between and within groups were sparse at 10%—each neuron in the sending group projected to each neuron in the receiving group with 0.1 probability (self-projections were not allowed).

These architectural details determine the network's capacity to propagate spikes from source to sink. The mean rate of spike propagation is further determined by the remaining free parameters of the network, and the average source voltage per unit time. If critical branching is a critical point between phases of decreasing versus increasing spike rates, then with respect to the aims of Simulation 1, these parameter settings should matter *only insofar as they co-determine a mean flow of spikes*. This claim is based on analyses from statistical mechanics showing that scaling laws become "universal" as systems approach given critical points. That is, the exponents of particular scaling laws approach theoretically derived values that do not depend on mechanistic details of the systems in question. Supporting this claim for the present model would require mathematical analyses and/or extensive sampling of the parameter space, both of which are beyond the present scope.

Instead, only two sets of parameter values were examined in Simulation 1, chosen to sample two distinct regions of the parameter space. One set was chosen to embody the broad assumption that neurons and synapses are heterogeneous, in that their parameter values vary considerably across neurons and synapses (Marder & Goaillard, 2006). Generic ranges for parameter values were chosen as defaults, and their values were initialized by sampling randomly from either uniform or exponential distributions. The other set was chosen to be homogenous, with variations only in the axonal delays, which are required for asynchronous dynamics.

For the heterogeneous set, membrane leak rate, spike threshold, and spike reset values were initialized randomly and uniformly in the ranges $0.1 < \lambda < 1.0$, $1.0 < \theta < 2.0$, $0.5 < \kappa < 1.0$, and $0.5 < \omega < 2.0$. These variables were then fixed during simulation runs, and informal tests indicated that results are robust to moderate variations their ranges. Refractory periods were held constant at one, and axonal delays τ_i were drawn randomly from an exponential distribution with a mean of 3.0. The exponential was used to simulate a wide range of delays, with fewer longer connections (i.e., longer delays) due to space constraints (Chklovskii, Schikorski, & Stevens, 2002). The probability ρ of enabling and disabling synapses was set to 0.05. This probability must be low to make the timescale of connectivity dynamics substantially slower than that of voltage dynamics. A separation of interacting timescales is an essential feature of self-organized criticality (Jensen, 1998), and it was necessary to obtain the results herein. For the homogeneous set, $\lambda = 0.1$, $\theta = 1.0$, $\kappa = 0.5$, $\omega = 0.75$, $0.5 < \tau < 1.0$, and $\rho = 0.05$. The upcoming results for heterogeneous parameters were not significantly different for the homogeneous set (not reported).

Source voltages were implemented as externally driven spikes on source neurons, and two source conditions were examined. In the *sequenced input* condition, source neurons were driven to fire in a precise order (neuron 1–40), cycling through all 40 neurons every two unit time intervals, with even spacing (0.05 time units) between successive source spikes. In the *Poisson input* condition, source neurons were driven to fire at random, with intervals between source spikes drawn randomly from an exponential distribution with a mean of 0.05. The sequenced condition is deterministic, and the Poisson condition is stochastic, but variations in the latter are restricted to timescales far below the predicted scaling laws, which should extend over thousands of time intervals and spikes. Therefore, for all but the smallest scales, extrinsic variations are absent under both source conditions, which means that scaling laws should be exhibited in the model's intrinsic variations.

Finally, STDP was implemented in a third, *Poisson + STDP* network by updating the weight on each enabled synapse of each neuron that spikes at each time t, using the following rules. For each enabled dendritic synapse, $\omega_t \leftarrow \omega_{t'} \pm \eta e^{-(t - t_{pre})}$, where t' is time of last weight update, t_{pre} is time of last spike on the presynaptic neuron, and η is a rate scale set to 0.01 herein. The second term is added for excitatory neurons (standard STDP) and is subtracted for inhibitory neurons (anti-STDP). For each enabled axonal synapse, $\omega_t \leftarrow \omega_{t'} \pm \eta e^{-(t - t_{post})}$, where t_{post} is time of last spike on the postsynaptic neuron, and the $\pm$ term is opposite the dendritic side. The use of anti-STDP for inhibitory neurons serves to strengthen inhibition when it comes shortly after spiking and is supported by studies of inhibitory interneurons (Holmgren & Zilberter, 2001).

Critical Branching Results

One million source spikes were input for each simulation. Critical branching was engaged for the first 700,000 source spikes and was disengaged thereafter. For the Poisson + STDP network, STDP was engaged for the entire simulation. Local σ_i estimates were tracked over the course of simulation by counting the number of spikes attributed to each neuron i (i.e., number of times its

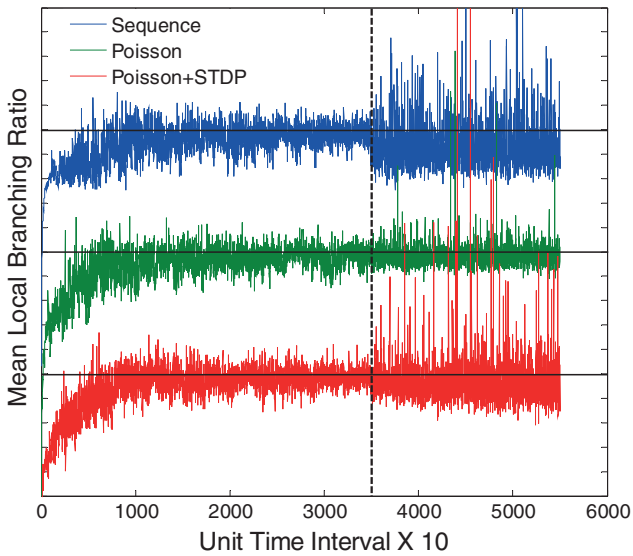

Figure 4. Time series of local branching ratio estimates (averaged over 10 unit time intervals per data point) for Simulation 1. Solid lines show ideal critical branching for each condition, and the dashed line shows when the critical branching mechanism was disengaged (spike timing dependent plasticity [STDP] remained engaged throughout).

axonal synapses were blamed) during each of its ISIs. $\langle\sigma\rangle$ is shown in Figure 4 for every 10 unit time intervals. $\langle\sigma\rangle$ starts at zero because synapses were initially disabled, and then gradually approaches and remains near one while the critical branching mechanism was engaged. After the mechanism was disengaged, $\langle\sigma\rangle$ dropped slightly (but still remained near one), and its variance increased substantially. These time series show that effective connectivity was set and maintained such that $\langle\sigma\rangle \sim 1$ while the critical branching mechanism was engaged, and after it was disengaged.

Evidence of $\langle\sigma\rangle \sim 1$ indicates that excitatory and inhibitory influences on spiking were balanced. To examine how this balance was struck, numbers and weights of enabled excitatory versus inhibitory synapses were examined after 700,000 source spikes. The results, shown in Table 1, indicate that the tuning mechanism worked consistently across the three network conditions. About 10 axonal synapses per excitatory neuron were enabled, and about three times as many were enabled per inhibitory neuron. The sum total of excitatory weight was less than half that of inhibitory weight. Greater inhibitory weight was needed to strike a balance between inhibitory and excitatory effects on spike propagation because of the disproportionate number of excitatory versus inhibitory units (about 3 to 1), coupled with roughly equal firing rates across units.

The excitatory/inhibitory balance was nearly perfect for excitatory units, as seen in σ estimates near one for excitatory units. However, spike propagation from inhibitory units was slightly subcritical, and the effect on spike propagation can be seen by comparing the rate of source spikes versus sink spikes. Perfect critical branching should perfectly preserve the flow of spikes from source to sink, thereby equalizing source and sink spike rates. The mean rate of source spikes in all conditions was 20 per unit time interval, but the mean rates of sink spikes were between 16 and 17 per unit time interval. These differences are accounted for by the fact that inhibitory units were slightly subcritical, which causes a small loss in spike propagation like an additional sink. The percentage below $\langle\sigma\rangle = 1$ roughly corresponds to the size of this small loss, which can be attributed to the rule for choosing synapses, because there is no loss when the rule is simply to choose synapses at random (not reported).

The three networks in Simulation 1 are roughly equivalent with regard to the measures presented thus far, despite different initial parameter values and input conditions, and despite the use of STDP in one network but not the others. While STDP did not affect net amounts of enabled excitation versus inhibition, it did affect the distributions of synaptic strengths, as can be seen in Figure 5. The sequence and Poisson conditions yielded similar patterns: There was a graded bias toward enabling smaller excitatory weights, given that weights were uniformly distributed over all synapses, but no such bias for inhibitory weights. This bias was due to the increased likelihood of going supercritical by triggering more spikes when synapses with larger excitatory weights are enabled, versus smaller weights.

The increased likelihood of going supercritical means that larger synapses are more likely to be disabled shortly after being enabled. No such bias occurs for inhibitory neurons because they do not trigger spikes. This bias can also be seen with STDP, but STDP caused weight values to move toward their minimum or maximum (for further explanation of this effect, see Song, Miller, & Abbott,

Table 1
Network Statistics for the Reservoir at Critical Branching in the Three Source Input Conditions Examined in Simulation 1

Network measure	Sequence		Poisson		Poisson + STDP	
	Excitatory 75%	Inhibitory 25%	Excitatory 75%	Inhibitory 25%	Excitatory 75%	Inhibitory 25%
Enabled synapses per axon	12.4	32.3	10.6	32.1	11.8	27.6
Sum weight enabled	4,323.2	9,733.3	4,601.4	10,002.2	4,578.7	9,330.0
Spikes per unit time	143.7 reservoir	45.0 reservoir	147.7 reservoir	49.0 reservoir	139.1 reservoir	49.3 reservoir
	16.3 sink		17.1 sink		17.1 sink	
Mean firing rate	0.190 reservoir	0.185 reservoir	0.197 reservoir	0.196 reservoir	0.186 reservoir	0.196 reservoir
	0.163 sink		0.171 sink		0.171 sink	
Branching ratio	0.988	0.921	0.994	0.931	0.996	0.944

Note. STDP = spike timing dependent plasticity.

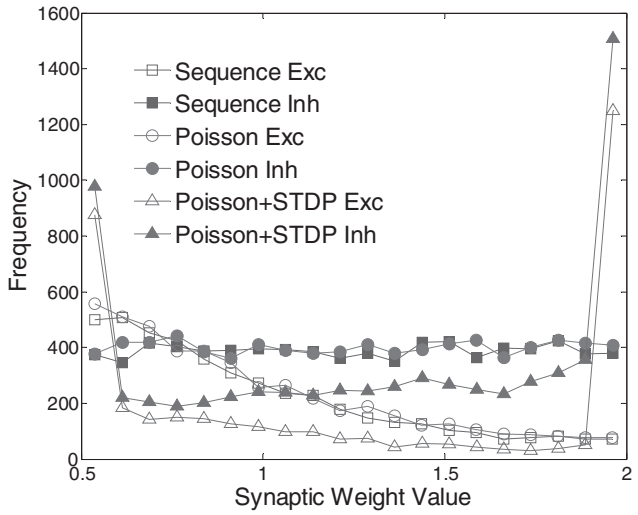

Figure 5. Distributions of synaptic weights for each of the three conditions in Simulation 1, plotted separately for excitatory (Exc) versus inhibitory (Inh) weights. STDP = spike timing dependent plasticity.

2000). Given that STDP was applied additively, consistent movement toward the boundaries caused weights to be concentrated at the boundaries. This distributional effect may be interesting in its own right, but for the present purposes, the effect serves to illustrate that critical branching is maintained under varying synaptic weight distributions by maintaining comparable numbers of excitatory and inhibitory synapses. These numbers yield comparable summed totals of excitatory and inhibitory weights.

Scaling Law Results

The results graphed in Figure 4 show that spike dynamics were actively maintained near their critical point, indicating that the critical branching mechanism contributed to variations in spiking. To test whether these contributions resulted in scaling laws, individual spike trains were examined first, examples of which are shown in Figure 6. One can readily see the heterogeneity of variation present in reservoir spikes that cannot be attributed to source variations. ISIs varied over a wide range of scales, and spikes clustered at multiple scales. The range of ISI variations can be expressed and analyzed via their probability distribution, and spike clustering can be expressed and analyzed via Allan factor analysis.

In Figure 7, ISI distributions are shown for one reservoir neuron in each condition, chosen to be representative of ISI distributions for other neurons in each condition. Each plotted neuron spiked at least once every 10 time intervals over a period of 10,000 time intervals. When the critical branching mechanism was engaged, distributions in all three conditions closely followed scaling laws roughly of the form $P(ISI) \sim 1/ISI^{\alpha}$, with $\alpha \sim 2.5$, regardless of source variability and STDP. Thus, tuning to critical branching produces ISI power law distributions similar to those reported for cat V1 and macaque IT recordings (Baddeley et al., 1997) and rat midbrain recordings (Bershadskii, Dremencov, Fukayama, & Yadid, 2001).

When the critical branching mechanism was disengaged, ISI distributions deviated from a power law and instead followed exponential-like distributions. ISIs have been associated with exponential probability distributions (Shadlen & Newsome, 1998) as well as power law distributions. However, relating the simulated results to empirical observations is complicated by other reports associating ISIs with bimodal (see Rowat, 2007), bi-exponential (Mazzoni et al., 2007), lognormal (Bershadskii et al., 2001), inverse Gaussian (Iyengar & Liao, 1997), and gamma (Robin et al., 2009) probability distributions. To simulate this range of results would require a level of model complexity beyond the present scope. The more general conclusion is that engaging the critical

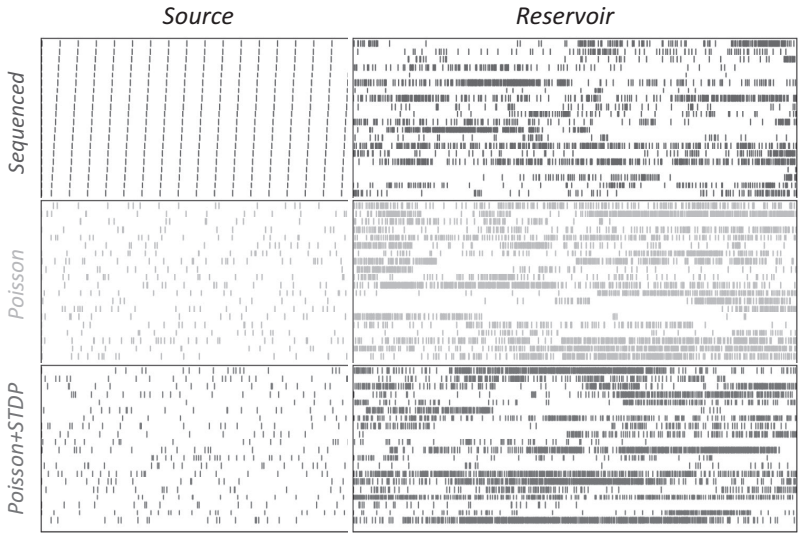

Figure 6. Twenty example spike trains from source neurons, and 20 from reservoir neurons, for each of the three different network conditions in Simulation 1, after estimated branching ratios asymptoted near critical. For clarity, source spike trains are shown at 20× temporal resolution compared with reservoir spike trains. STDP = spike timing dependent plasticity.

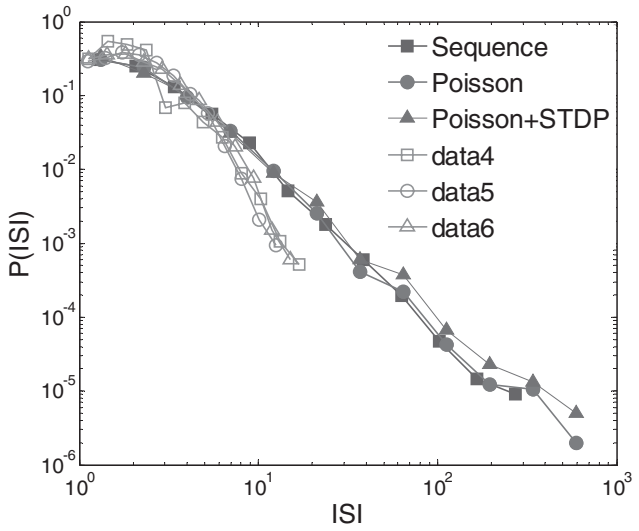

Figure 7. Interspike interval (ISI) distributions for the three network conditions in Simulation 1, plotted while the critical branching mechanism was engaged (filled symbols) versus disengaged (unfilled symbols). In both cases, estimated branching ratios had asymptoted near critical. Histogram uses logarithmic binning so that count estimates are evenly spaced on a log scale. STDP = spike timing dependent plasticity.

branching mechanism results in high ISI variability, for example, in terms of heavy-tailed distributions and coefficients of variation > 1. Such high ISI variability is commonly found in single-cell recording studies (Softky & Koch, 1993; Troyer & Miller, 1997).

Going beyond ISI distributions, one can ask whether there are dependencies across sequences of ISIs. Studies of temporal dependencies in spike trains have consistently found long-range correlations spanning multiple timescales (Bhattacharya, Edwards, Mamelak, & Schuman, 2005; Gerstein & Mandelbrot, 1964; Jackson, 2004; Rasouli et al., 2006; Teich et al., 1997). An established method for examining temporal correlations in spike trains is the Allan factor, which has advantages over similar methods like the Fano factor (Teich & Lowen, 1994). The Allan factor, $A(T)$, measures a scaling relation between window size and deviations in spike counts within adjacent time windows. In particular,

$$A(T) = \frac{\langle [N_i(T) - N_{i+1}(T)]^2 \rangle}{2\langle N_i(T) \rangle},$$

where $\langle N_i(T) \rangle$ is expected spike count in each window i of size T (sampled in powers of 2), and i indexes adjacent windows tiled over a given spike train. Teich and colleagues (Teich et al., 1997; Teich & Lowen, 1994) found that spike trains from both auditory and visual systems of the cat exhibit two regimes of effect. At the shortest timescales, spike trains are well-described by a Poisson process, for which $A(T) \sim 1$, and no scaling relation holds. However, at longer scales, $A(T)$ goes as $A(T) \sim T$, which is the point process equivalent of 1/f scaling in spectral analysis (see below).

Allan factor analyses are shown in Figure 8. All three model conditions exhibited the same basic pattern of results: Model spike trains exhibited the two regimes observed empirically, where spikes were Poisson-like at smaller scales and were scaled with T at larger scales. Engagement of the critical branching mechanism was necessary for this result, because spike trains were Poisson-like over all scales when the mechanism was disengaged. To show that this result was not purely due to power law distributed ISIs, spike trains were shuffled randomly so as to preserve their ISI distributions, and Allan factor analyses of the resulting surrogates showed a more unitary scaling relation with an exponent roughly half that of the unshuffled spike trains.

Next, let us consider temporal correlations over summations of spikes across neurons. Summations are indirectly related to local field potentials, electrophysiological recordings, and behavioral movements. Intrinsic variations in these measures are expressed as time series of measurements that either directly or indirectly reflect spike counts over adjacent time windows, and such time series have been found to exhibit long-range temporal correlations (for a review, see Kello et al., 2010). There are numerous methods for analyzing such correlations (see Farrell, Wagenmakers, & Ratcliff, 2006; Rangarajan & Ding, 2000), but the present study only aims to establish that the critical branching mechanism yields a 1/f-like scaling relation similar to those observed empirically.

Time was sliced into unit time intervals and spikes per interval were counted over all reservoir neurons. The resulting time series for each model are shown in Figure 9. Spike counts ramped up as the networks approached critical branching and exhibited fluctuations over a wide range of temporal scales while the critical branching mechanism was engaged. Wide-range fluctuations disappeared once the mechanism was disengaged. Spectral analysis was applied to two segments of each spike count series, as shown in Figure 10, where each segment was 2^{13} counts in length. The first segment of each series ended just prior to the disengagement of critical branching, which was after reaching asymptote. The

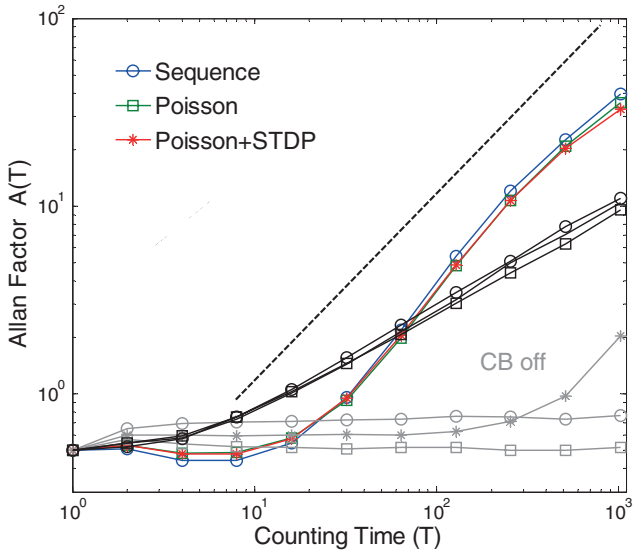

Figure 8. Scaling of the Allan factor, $A(T)$, with window size T, for spike trains from Simulation 1. Allan factors are shown with critical branching (CB) engaged and asymptoted (colored series), with CB disengaged (gray series), and with interspike intervals from the colored series shuffled (black series). Dashed line shows a slope of 1. STDP = spike timing dependent plasticity.

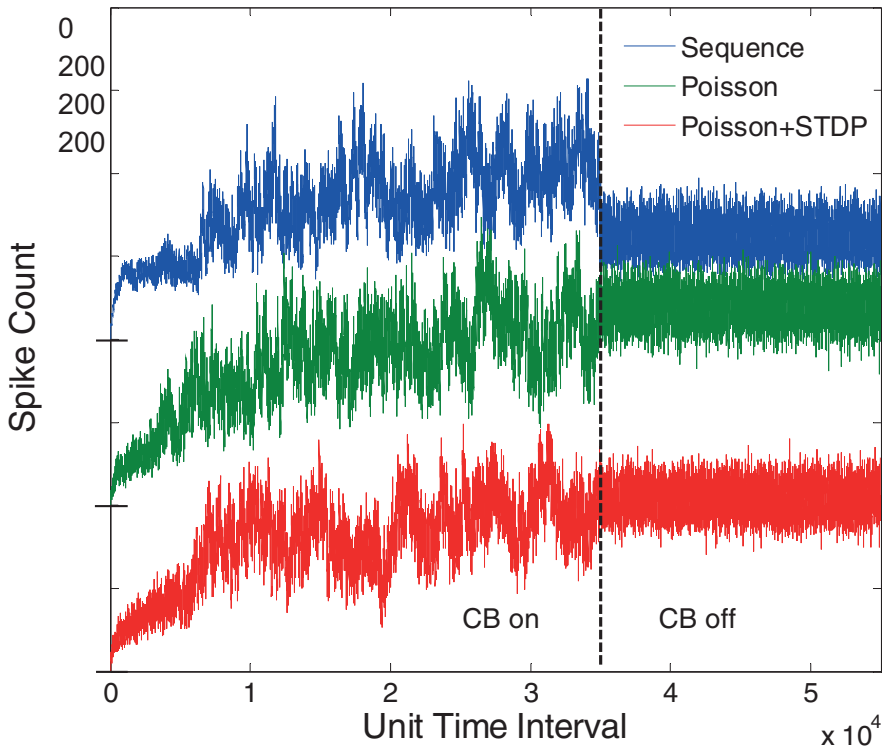

Figure 9. Time series of spike counts in unit time intervals, for each of the three conditions examined in Simulation 1. The dashed line shows when the critical branching (CB) mechanism was disengaged. STDP = spike timing dependent plasticity.

second segment of each series started 5,000 time intervals after disengagement.

For all network conditions when critical branching was engaged, the spectra show a clearly lawful 1/f scaling relation in the lower frequencies, where the lion's share of spike count variance resides. Higher frequencies were characterized by uncorrelated fluctuations. This combination of 1/f-like and uncorrelated fluctuations is the typical finding in studies of intrinsic neural activity (Mazzoni et al., 2007). When critical branching was disengaged, the low frequency 1/f scaling relations were replaced by uncorrelated plateaus, plus steeper, $1/f^2$-like scaling relations in the mid-range frequencies. Most empirical studies of 1/f-like scaling in neural

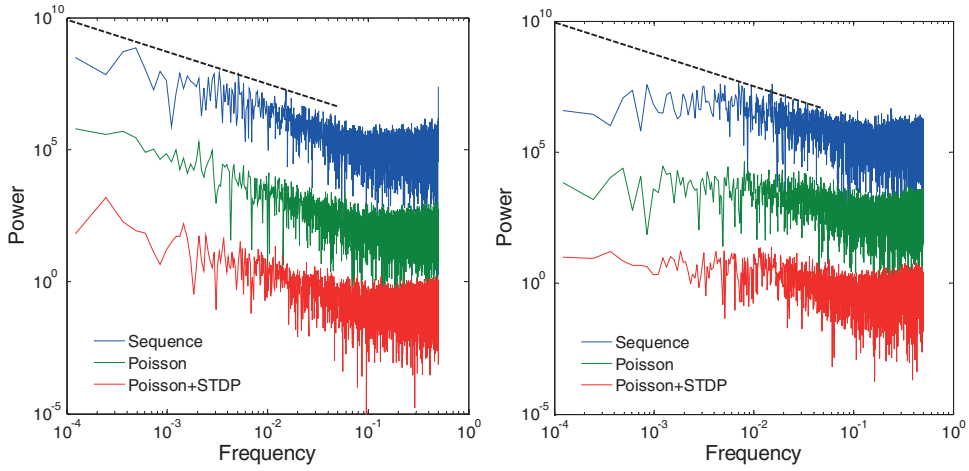

Figure 10. Power spectra for the series of spike counts shown in Figure 9, with and without the critical branching mechanism engaged (left and right graphs, respectively). The dashed line shows ideal 1/f scaling. STDP = spike timing dependent plasticity.

activity do not use sophisticated methods for comparing data against 1/f scaling versus alternate statistical models (e.g., see Thornton & Gilden, 2005). The present claim is only that simulation results resemble empirical results. As alternate models are proposed in the future, it will be important to use model testing methods to determine which provide best explanations of the data.

The Allan factor and spectral analyses show clearly that engagement of the critical branching mechanism was necessary to produce scaling laws in spike dynamics, whereas its engagement was not necessary to produce the ISI power law distributions. The fourth and final scaling law to be examined is the neuronal avalanche, which is a power law distribution at the network scale, instead of the individual spike train. The avalanche is generally a burst of neural activity, such as a contiguous time period during which LFPs are above some threshold (Beggs & Plenz, 2003), and avalanche size is essentially the sum of activity within a given above-threshold period. Avalanche analysis is typically applied when activity is inherently composed of bursts (but see Montez et al., 2009), and results show that avalanche sizes go as $P(S) \sim S^{-\alpha}$, where $\alpha \sim 3/2$. The particular exponent value is predicted for critical branching processes and is related to generic aspects of information transmission and storage in network activity (Beggs, 2008).

The spiking model parameters used thus far are not well-suited to bursts of spiking activity because the source spike rate is high enough to generate a flow of spikes that fluctuates around a mean well above zero. To simulate bursts of spiking activity off a floor near zero, the rate of source spikes was decreased to only 5% of the rate used in simulations presented thus far. To compensate for fewer tuning/learning opportunities, the tuning and STDP learning rates were multiplied tenfold. All other parameters were unchanged. The resulting bursts of spiking in reservoir neurons are evident in the example series shown in Figure 11. The start of each burst was defined by crossing a threshold of > 1 reservoir spike per time interval, and each burst ended when spikes per interval fell back below threshold. Burst sizes were gathered over 10,000 intervals of bursting activity after networks asymptoted near critical branching.

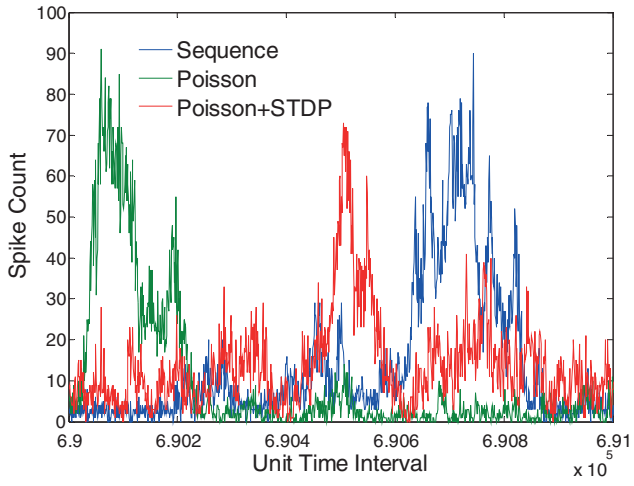

Figure 11. Time series of spike counts in unit time intervals, when the flow of Poisson spike inputs was 20× less than that for other Simulation 1 results. STDP = spike timing dependent plasticity.

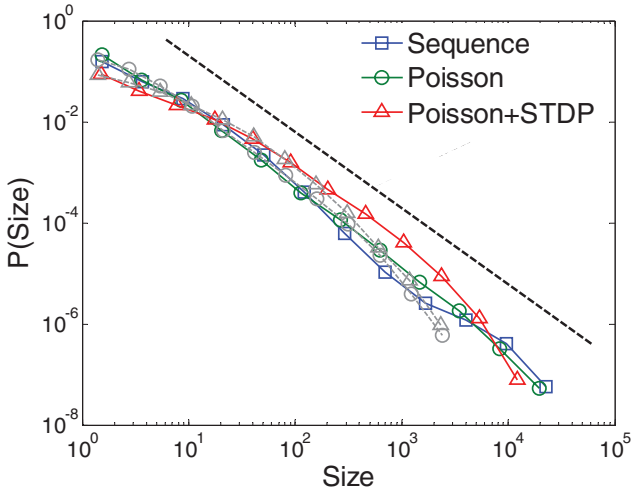

Figure 12. Neuronal avalanche distributions for the three different model conditions while critical branching was engaged (colored series) versus disengaged (gray series). With regard to the latter, avalanches in the Sequence condition were highly stereotyped and, hence, were not distributed over a significant enough range of sizes to be plotted. The dashed line shows the ideal –3/2 slope predicted by critical branching. STDP = spike timing dependent plasticity.

The distributions of burst sizes for each network condition are plotted in Figure 12 in logarithmic coordinates, separated by when critical branching was engaged versus disengaged. The graph shows that most burst distributions closely followed a scaling relation with the predicted and observed 3/2 exponent (see Mazzoni et al., 2007). The inclusion of STDP caused the distribution to bend slightly away from a power law and toward and exponential distribution, and a slighter bend was observed when the critical branching mechanism was disengaged (the range of burst sizes was more restricted in this case as well). This bend is present in some empirical studies of neuronal bursting (e.g., Beggs & Plenz, 2003) and is at least partly due to mundane limitations in recordings and model size. The general conclusion is that burst sizes resembled the observed distributions known as neuronal avalanches. This was most true when the critical branching mechanism was engaged, suggesting that results were obtained by virtue of being near a critical point.

In summary, Simulation 1 results established the effectiveness of the critical branching mechanism and accounted for a wide range of observed scaling laws in spiking activity. Estimated exponents of model scaling laws were consistent with those of empirical data—3/2 for neuronal avalanches and 1 for temporal correlations in Allan factor and spectral analyses—as predicted for systems near order/disorder critical points. Other neuronal models of 1/f scaling not based on criticality, like Davidsen and Schuster's (2002) model, do not readily explain observed exponents, have not been shown to exhibit neuronal avalanches, and have not been related to cognitive function (Simulation 2) or behavior (Simulation 3).

Scaling laws in ISI distributions and temporal correlations occurred only while the critical branching mechanism was engaged, including the Sequenced condition in which the only source of noise was the stochastic enabling and disabling of spikes. Thus, 1/f

scaling did not emerge from explicit brown noise, as in some models (e.g., Davidsen & Paczuski, 2002). For neuronal avalanches, scaling law distributions occurred regardless of whether the critical branching mechanism was engaged or disengaged, once branching ratios had asymptoted near critical. This result suggests that the pattern of connectivity determined by critical branching was a factor in generating neuronal avalanches, but it may be that more generic connectivity patterns would also produce these distributions. This ambiguity was addressed by examining spike activity for two kinds of generic, surrogate connectivity patterns.

For one kind of surrogate, critical branching connections were scrambled such that the numbers and weights of outgoing connections were preserved for each excitatory and inhibitory neuron, but the neurons they projected to were randomized. These scrambled networks became supercritical and did not exhibit power law distributions, despite preserving the total amounts of excitatory and inhibitory inputs. Therefore the observed power law distributions arose from the particular pattern of projections determined by critical branching, which governed the timing of excitatory and inhibitory inputs to neurons. For the other kind of surrogate connectivity, networks were connected randomly with mean numbers of enabled synapses equal to those found in critical branching networks. Connections weights were then randomized to values that resulted in spiking rates roughly equal to those in critical branching networks. These surrogate networks also failed to exhibit neuronal avalanches, exhibiting exponential-like distributions instead. Thus, a randomized, rough balance of excitation and inhibition does not appear to be sufficient to account for neuronal avalanches—along with the other scaling laws, simulated neuronal avalanches can be attributed specifically to the critical branching mechanism.

Simulation 2: Critical Branching and Computational Capacity

Results of Simulation 1 indicate that homeostatic tuning toward critical branching can explain a range of scaling laws observed in neural activity. The critical branching mechanism promoted a dynamic balance of excitation and inhibition such that each spike was blamed on average for one spike moving forward in time, except for spikes on sink neurons. This balance is adaptive in terms of conserving spikes, but what is the role of critical branching in perceptual and cognitive functions, broadly speaking? It may maximize information transmission in terms of spike propagation (Hsu & Beggs, 2006), but functions of learning, memory, and perception require encoding and transformation of information over time.

Homeostatic tuning is not learning, in that the objective is not to represent or associate spike inputs over long timescales. However, recurrent networks can naturally and inherently encode spike inputs over short to mid-range timescales, in the range of milliseconds to seconds and minutes. Even randomly connected networks may have memory in the sense that a pattern of spike activity at one instant will carry information about past inputs. If network dynamics are nonlinear, inputs may be richly encoded such that nonlinear classifications are possible on the basis of linear separations of spike patterns. If these memory and encoding capacities are enhanced by critical branching, then the principle may directly support cognitive functions without explicitly representing or associating spike inputs. Information could be extracted by "readout" networks that learn to decode the spike dynamics of generic recurrent networks tuned to critical branching.

As mentioned earlier, this approach to analyzing and theorizing neural networks is known as reservoir computing. Reservoir computing studies have shown that fading memory and nonlinear separability properties of reservoirs are maximized when tuned to a critical point between ordered and chaotic dynamics, as gauged by linear readout functions (Bertschinger & Natschlager, 2004). Critical branching strikes the same kind of balance with respect to spike dynamics, instead of threshold gate dynamics as examined previously. If being near this critical point is similarly adaptive, then critical branching should have the same maximizing effect. Note that such maximization does not entail optimization of any particular objective function, although it may support balanced performance across a wide range of objective functions (there is no free lunch in optimization; Wolpert & Macready, 1997).

The computational properties of critical branching reservoir dynamics were tested by adopting techniques used in previous reservoir computing studies. Spiking network models were built as in Simulation 1, with the main difference being in the distributions of source inputs. The sequence condition used previously was modified so that, instead of one repeated sequence of spikes, there were two possible sequences that represented the two possible values of a "bit" input (see Figure 13). One sequence, say bit value 0, was presented over source neurons 1–20, and the other was presented over source neurons 21–40. Each sequence consisted of 20 spikes evenly spaced over one unit time interval. For each time interval, a bit sequence was chosen at random to be presented to the network. Over time these random bit inputs created a flow of spikes from source to sink via the reservoir. Tuning was engaged as before, and LIF parameters were adjusted to encourage sparse effective connectivity. Previous investigations (Kello & Mayberry, 2010) showed that memory and encoding capacities are generally greater for sparse networks, presumably because of reduced variability in spike pattern trajectories. These parameter changes had no appreciable effects on scaling laws (not reported).

Memory and encoding properties of the reservoir were assessed by taking a snapshot of the reservoir spike pattern at each unit interval *t*, and using reservoir patterns as the predictor variables for

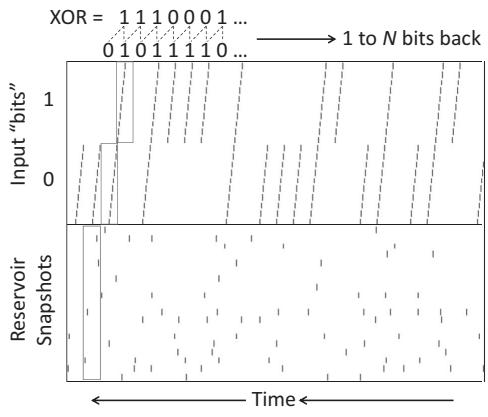

Figure 13. A sample sequence of 25 random bit values (outlined rectangles), each represented as a sub-sequence of source spikes, and the corresponding spikes for a random sampling of reservoir neurons.

linear regression equations. The variables being predicted were nonlinear functions of past input bits at times, that is, XOR functions of bits at times *t*-N and *t*-N-1. The memory capacity of the reservoir was thus assessed by the encoding of past bits in each current spike pattern, and the encoding capacity was assessed by the ability to perform nonlinear computations on past bits using only a linear separation of reservoir spike patterns. These capacities were assessed after disengaging the tuning mechanism in order to hold connectivity constant. Given that refractory periods were one unit interval in length, each reservoir spike pattern could be represented as a binary vector indicating the presence or absence of a spike for each reservoir neuron. Spikes were actually timed more precisely, but this precision was discarded to more closely mimic prior reservoir computing methods. Ordinary least squares linear regression was then used to compute the XOR function on adjacent bits N and N-1 time intervals *in the past*, with a separate set of coefficients computed for each N.

The general pattern of results replicated prior work on reservoir computing with spiking neuron models, often referred to as *liquid state machines* (Maass et al., 2002). XOR accuracy was near perfect for the most recent bits and fell off gradually over time till reaching chance performance (see Figure 14). Thus, reservoir spike dynamics had a fading memory that projected inputs into higher dimensional spaces useful for nonlinear functions like XOR, analogous to nonlinear support vector machines. However, more to the point, critical branching maximized memory and encoding capacities, as measured by mean accuracy over time. This maximum is by comparison with two methods for deviating from critical branching.

One method of deviation was to engage the tuning mechanism but bias the probability ρ of enabling versus disabling synapses. In particular, synapses were enabled and disabled with probability $\rho\beta$ and ρ/β, respectively, where $\beta < 1$ led to $\langle\sigma\rangle < 1$, and $\beta > 1$ led to $\langle\sigma\rangle > 1$. As shown in Figure 14, mean accuracy was maximal at critical branching, that is, unbiased $\beta = 1$. The other method of deviation was to enable excitatory and inhibitory synapses at random, without use of the tuning mechanism, such that the mean rate of reservoir spikes was approximately equal to that during critical branching. Again, mean accuracy was well below critical branching.

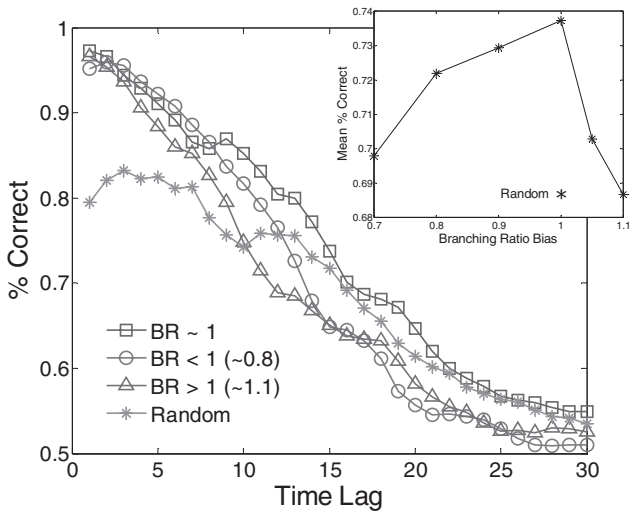

Figure 14. Classification accuracy using a linear readout of reservoir spike vectors. Given a spike vector at time t, accuracy is plotted as a function of computing the XOR function on input bits N and N-1 time intervals in the past, for four different branching ratio (BR) conditions: critical (BR $\sim$ 1), subcritical (BR $<$ 1), supercritical (BR $>$ 1), and a reservoir with randomly enabled synapses (Random). The inset shows mean accuracy as a function of BR bias (where 1 is unbiased, i.e., critical).

In summary, the reservoir computing analyses show how critical branching can be beneficial to cognitive functions, broadly speaking. Spikes are fleeting in comparison with the multiple timescales of perception, action, and cognition. For instance, while most stimuli and movements have behaviorally relevant dynamics on the order of milliseconds, their dynamics also exhibit structured patterns over seconds, minutes, and much longer timescales. Spike dynamics must have memory if they are to encode sensory and motor patterns over longer timescales, and this encoding must be rich enough to support nonlinear mappings among different pattern domains. Reservoir analyses show that critical branching can enhance this kind of memory and encoding capacity in recurrent networks of LIF neurons.

Simulation 3: Critical Branching and Behavioral Fluctuations

To model specific perceptual and cognitive functions, one needs to go beyond the generic reservoir computing results presented in Simulation 2. The most incremental step would be to incorporate linear classification as a spiking "readout network" that uses learning mechanisms to make linear discriminations among reservoir patterns, or associate them with target patterns. Readout networks could be useful constructs, but random, generic reservoirs may be limited in their ability to explain neural and cognitive function. It may be necessary for learning to shape recurrent networks to fit observed distributions over sensory inputs, for instance, or to make associations between actions and rewards (see Friston, 2010).

Simulation 1 demonstrated the efficacy of critical branching while synaptic weights are adjusted by STDP, but it remains to be seen whether critical branching would interfere with learning or memory processes supported by STDP or other Hebbian-like mechanisms. Assuming that interference could be avoided, how would actions of the critical branching mechanism manifest in behavior? The answer is that critical branching should yield scaling laws in the intrinsic variations of behavioral activity, as it does in neural activity. The means by which neural and behavioral variations are linked is an ongoing area of investigation, but a general prediction can be made: If critical branching pervades neural activity, then 1/f scaling laws should pervade measures of intrinsic fluctuations in behavior. Consider the following two studies on pervasive 1/f scaling in behavior, and how critical branching can account for their results.

In one study, participants repeated the word "bucket" and fluctuations in acoustic energy across repetitions were analyzed as a function of acoustic frequency (Kello et al., 2008). Results showed numerous 1/f fluctuation series that were mutually uncorrelated, and ran in parallel through the repetitions of each syllable (Kello, 2011; Moscoso del Prado Martín, 2011). It was argued that these results required too many isolable sources of 1/f scaling for them

to be plausible, because one would need a new source for each distinct 1/f series. The preferred alternative is that 1/f scaling is general and pervasive to intrinsic fluctuations, in that the same explanation applies to all measured sources.

Critical branching is one such explanation, because scaling laws are explained by a mechanism that affects interactions among neurons through enabling and disabling synapses. Thus, 1/f scaling caused by homeostatic tuning to critical branching is explicitly predicted to be pervasive, on the premise that such tuning is widespread throughout nervous systems. How would homeostatic tuning be reflected in behavior to yield pervasive 1/f scaling in behavioral measurements? One answer is readily available in a simple, behavioral interpretation of results from Simulation 1.

Recall that 1/f fluctuations were found in spike count time series, where spikes were counted across reservoir neurons per unit time interval. If these neural networks were shaped to drive the articulatory motor system, then one could relate the strength of muscle contraction to spike rates across motor neurons. Evidence for a rate code relation between motor neural activity and movement is well-established (Brooks, 1986), even if spike timing also plays a role (Rieke, Warland, van Steveninck, & Bialek, 1996; Stein et al., 2005). This evidence supports a link between neural and behavioral 1/f fluctuations via critical branching, but how can this link explain parallel, distinct 1/f fluctuations in behavior?

Two answers to this question are offered. For acoustic fluctuations in spoken word repetitions, the most straightforward answer is that different articulatory degrees of freedom are served by different neural networks. In order to account for the results, networks must be sufficiently distinct such that neural activity in one network is independent or only loosely coupled to activity in other networks (e.g., only partially overlapping). Spike rate fluctuations driven by homeostatic tuning to critical branching would then yield parallel, distinct 1/f fluctuations in the acoustic manifestations of articulatory degrees of freedom. It is beyond the present scope to build a neural network model of spoken word production that can simulate articulatory trajectories like "bucket," and it would be gratuitous to simply build a set of independent or loosely coupled reservoir networks—Simulation 1 already establishes an outcome of parallel, distinct 1/f fluctuations. Therefore critical branching provides a firm basis for building models of speech production that would account for Kello et al.'s (2008) results.

The second way to explain parallel, distinct 1/f fluctuations in behavior is illustrated by the second study of pervasive 1/f scaling mentioned earlier. Kello et al. (2007) investigated the effects of cue predictability on 1/f scaling in series of simple and choice responses. To test for pervasiveness, they measured not only series of response times, but also series of time intervals between each key-press and key-release, that is, key-contact durations. Response times and key-contact durations each exhibited distinct 1/f fluctuations that were uncorrelated with each other. Moreover, the predictability of response cues decreased the estimated 1/f exponents in response times toward random, white noise fluctuations. By contrast, 1/f exponents in key-contact durations were unaffected by cue predictability. These key-press data add another dimension to testing pervasiveness because the effects of stimulus predictability were dissociated between response times and key-contact durations.

For Simulation 3, two measures of spiking activity were formulated under conditions that abstractly simulate receiving and responding to stimuli. The stimuli are pulses of source spikes intended to simulate the response cues from Experiment 1 of Kello et al. (2007). Two dependent measures were formulated to be distinct from each other, and analogous to key-press response times and durations. These measures captured the essential feature that response times and durations are defined relative to stimulus onset, but otherwise they did not simulate motor processes or kinematics. The aim was to investigate whether a critical branching network could simulate two parallel series of response measures that exhibit independent, dissociable 1/f fluctuations.

In the experiment, a series of key-presses were elicited in response to series of simple visual cues—repeated appearances of "X" on a blank screen. Cue intervals were constant in one condition and were drawn randomly from an exponential distribution in another condition. Thus, cues were either predictable or unpredictable, respectively. In the simulation, the Poisson source condition from Simulation 1 was modified to alternate between a background mean rate of 10 spikes per unit time interval, and a cue rate of 100 spikes per time interval. Each cue was one time interval in duration, and a cue was presented once every 50 time intervals in the predictable cue condition. In the unpredictable condition, intercue intervals were sampled randomly from an exponential distribution with a mean of 50 and a minimum of 20. Example series of source pulses are shown in Figure 15, along with corresponding fluctuations in reservoir and sink spikes. Network parameters were as in Simulation 1, except 100 source units were used instead of 40.

A simulated response was triggered when the reservoir spike rate increased beyond a given threshold. This method of linking neural activity with reaction times is based on previous studies associating spike rates with accumulation of noisy stimulus information (Smith & Ratcliff, 2004). In particular, changes in spike rate were measured by tracking two ISI running averages at two different timescales, each one calculated as $ISI_{avg} = \beta ISI_i + (1 - \beta)ISI_{avg}$, where $\beta_{long} = 0.0005$, and $\beta_{short} = 0.005$ for the longer and shorter timescales, respectively. When $ISI_{ratio} = ISI_{long\_avg}/ISI_{short\_avg}$ exceeded 1.5, a stimulus was detected. A response was then simulated as being detected when ISI_{ratio} fell below 1.4, and response time was the time of response detection minus the time of stimulus onset. Response duration was simulated by a measure of the time needed for a set number of spikes to flow through the network after response initiation. In particular, the time it takes for 100 spikes to flow to the sink after 400 spikes have flown through the reservoir post stimulus-detection. These parameters were the best found in accounting for the data, but moderate variations yielded the same basic pattern of results.

Ten models were run for 100,000 time intervals with predictable cues, and 10 models with unpredictable cues. Critical branching tuning remained engaged throughout, and the last 1,024 responses were analyzed for each model, well after branching ratios had asymptoted near one. Distributions for simulated response times and durations were both Gaussian with positive skew, as with empirical data. Correlation analyses showed that response times and durations were only weakly correlated, mean $r = .21$ and .26 for predictable and unpredictable cues, respectively. Weak, unreliable correlations were found in the empirical data, consistent with evidence of dissociations in their spectra. The same dissociation

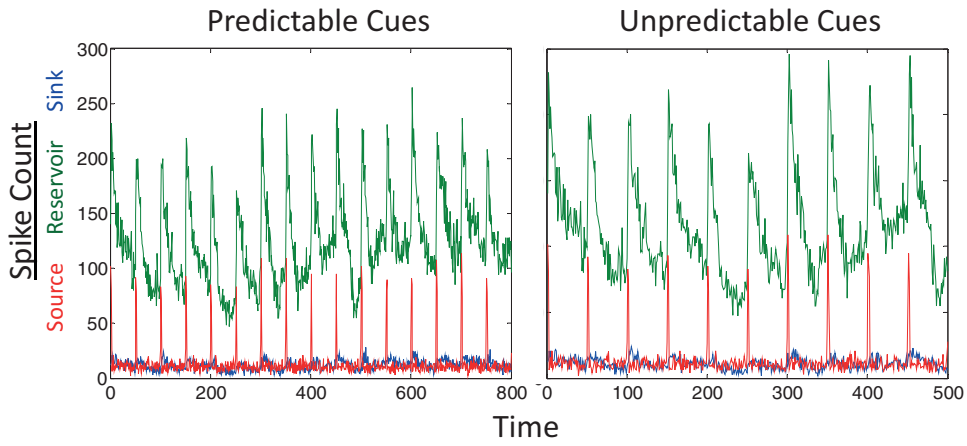

Figure 15. Example spike count series from Simulation 3, for source and reservoir spikes in both predictable and unpredictable cue conditions.

was exhibited by the model, as shown by the averaged spectra in Figure 16—cue predictability affected the 1/f scaling relation in response times but not response durations. This dissociation was examined the same way as in Kello et al. (2007), that is, by fitting regression lines to the lower 50% of the individual model spectra, and then performing *t* tests on the slopes. Slopes for response times to predictable cues were steeper than those to unpredictable cues, $M = -0.64$ versus -0.40, $t(9) = 7.3$, $p < .0001$, whereas cue predictability had no reliable effect on slopes, $M = -0.73$ and -0.68, $t(9) < 1$. Also, overall slope values were approximately the same between simulation and empirical data.

In summary, critical branching can account for pervasive 1/f scaling in the intrinsic fluctuations of human behavior, as expressed in spoken word repetitions and key-press responses. With regard to the latter, Simulation 3 went beyond Simulation 1 in demonstrating 1/f scaling in two additional measures of spiking activity, and a 1/f dissociation in the effect of cue predictability. This dissociation was simulated *not* because of dissociable mechanisms, but because of pervasive 1/f fluctuations. Pervasiveness means that dissociations are predicted for any mutually independent measures of intrinsic fluctuations. More detailed accounts require more detailed behavioral models, for example, for simple and choice response tasks. Simulation 3 is proof-of-concept that critical branching networks may provide a basis for such models.

General Discussion

The present study began with the aim of modeling scaling laws in the intrinsic variations of neural and behavioral activity. This aim was motivated by the ubiquity and pervasiveness of scaling laws, but also by previous studies suggesting links between scaling law variations, and neural and cognitive functions. Some of these previous studies were theoretical, in that they related computational capacity with critical points near second-order transitions between ordered and disordered phases (Bertschinger & Natschlager, 2004; Kwok & Smith, 2005; Langton, 1990; Packard, 1988). Other previous studies demonstrated empirical associations between effects on perceptual and cognitive processing, and cor-

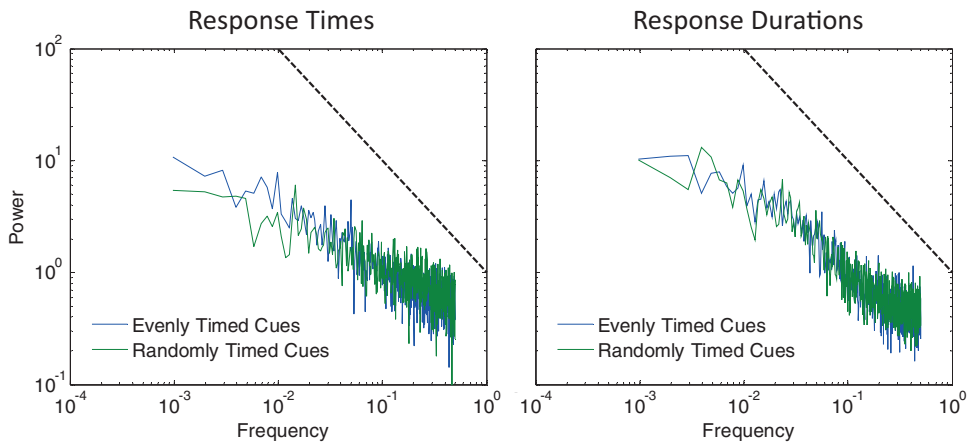

Figure 16. Spectral analyses of response time series and duration series from Simulation 3, plotted separately for predictable versus unpredictable cues. Dashed lines show $1/f^{ex=1}$.

responding effects on scaling laws in neural and behavioral activity (Ding, Chen, & Kelso, 2002; He, Zempel, Snyder, & Raichle, 2010; Holden, Choi, Amazeen, & Van Orden, 2011; Kello et al., 2007; Linkenkaer-Hansen, Nikulin, Palva, Kaila, & Ilmoniemi, 2004). Still other studies have demonstrated relations between breakdowns in scaling laws, and breakdowns in neural and cognitive function (Gilden & Hancock, 2007; Hobbs, Smith, & Beggs, 2010; Linkenkaer-Hansen et al., 2005; Montez et al., 2009).

Critical branching neural networks provide a basis for tying together these and other previous studies, and relating them to homeostatic and computational functions. Previous studies have demonstrated relations between critical branching and neuronal avalanches, and between criticality and computational capacity. The model and simulations herein goes beyond previous studies by drawing explicit connections between critical branching, a more diverse range of scaling laws, computational capacity, and behavioral data. To the author's knowledge, no single model has heretofore simultaneously accounted for fractal spike train clustering, neuronal avalanches, and 1/f scaling. Nor has prior research related all these scaling laws in spike dynamics to maximal computational capacity. In providing the first simulation of dissociable 1/f scaling in behavior, the present work may help spur further dialog between models and observed manipulations of power laws in behavior. Individual power laws may always find multiple alternative explanations, but observed pervasiveness and experimental effects constrain the number of possible explanations. To date, only critical branching has demonstrably satisfied these constraints.

The contribution of critical branching to our understanding of power laws in neural and behavioral activity can be expressed in terms of Marr's (1982) three levels of analysis. At the computational level, critical branching is a homeostatic goal that researchers have hypothesized to exist as a principle of neural and cognitive function. This principle is couched within the broader framework of self-organized criticality (Bak, Tang, & Wiesenfeld, 1987), which states that critical points are attractors of many complex systems. At the algorithmic level, the homeostatic tuning mechanism was designed to work with neural network models where spikes flow from source to sink. This conceptualization of spiking networks is unique in cognitive science, and general enough that one could apply it to any model where events propagate among nodes, and propagation needs to be regulated by adjusting connectivity. At the implementational level, the tuning mechanism was built with as little neural machinery as possible, and as consistently as possible with current neuroscience evidence.

The present results raise many questions and issues, from multiple perspectives. The remainder of this article considers a number of perspectives from various disciplines, along with the questions and issues they raise. These perspectives place the model in a broader context for interpreting results thus far, and they help illuminate the model's limits and potentials.

From the perspective of physics, it would help to show more rigorously the model parameterizations that yield critical branching and the associated scaling laws. The claim is that parameters need only support a flow of spikes from source to reservoir to sink, where low versus high flow rates yield bursts versus fluctuations in spike activity. The timescale of synaptic enabling and disabling (as governed by the probability ρ) need only be substantially slower than that of membrane and action potentials. These claims of generality derive from work on critical points and their associated scaling laws, and further analyses are needed to support them.

Another question from physics is whether the flow from source to sink means that thermodynamic principles can be applied (Swenson & Turvey, 1991). This flow has at least a surface similarity to heat transport in non-equilibrium thermodynamics, as illustrated by the Rayleigh–Bénard preparation. Oil molecules move from the heat source (bottom of the pan) to its sink (oil surface at top) to dissipate their energy, thereby increasing entropy according to Boltzmann's second law of thermodynamics. Similarly, spikes dissipate excitation by propagating from source to sink via the reservoir, although it not clear whether entropy can be defined in a thermodynamic sense. Also, when a critical temperature difference between source and sink is obtained, oil molecules self-organize into Rayleigh–Bénard convection cells that more quickly dissipate heat. In the model, spikes circulate in "eddies" of sorts, and dissipate in bursts or fluctuations as source excitation is increased. Further work is needed to investigate the roles of source excitation and sink dissipation on scaling law pattern formation in spike dynamics.

From the perspectives of computer and information sciences, one would like to know how model parameters interact with critical branching to affect the computational capacities of spike dynamics. It was mentioned earlier that these capacities are generally increased when synapses are only sparsely enabled. The critical branching mechanism yields sparsely enabled synapses when there is a high probability that each excitatory PSP will trigger a spike. Therefore, model parameters will enhance computational capacities to the extent that they afford high "spike trigger" probabilities. Further work is needed to investigate other factors that might affect computational capacity, such as the structure of potential connectivity and the pattern of source excitation.

Another question from computer and information sciences is whether the memory and encoding capacities of spike dynamics might approach an information theoretic limit. Poisson distributed ISIs have maximal Shannon entropy and hence maximize the possible bits of information carried by an individual spike train (Rieke et al., 1996). Model spike trains approached this limit after spike propagation asymptoted near critical branching and the tuning mechanism was disengaged. Spike timing was uncorrelated as shown by Allan factor analyses, and ISI distributions were exponential. However, the tuning mechanism caused spike trains to exhibit lower Shannon entropy due to the statistical, nested regularities of scaling laws. It would be interesting to investigate whether memory and encoding capacities might be associated with maximizing such regularities across scales, rather than approaching an information theoretic limit.

With respect to the information capacity of spike patterns across neurons, Fisher information analyses of linear reservoir models with Gaussian inputs suggest that there may be significant limits on reservoir capacities (Ganguli, Huh, & Sompolinsky, 2008), although sparse input conditions and nonlinear reconstruction may allow networks to go beyond these limits (Ganguli & Sompolinsky, 2010). The limits of reservoir computing models stem from their fading memory property, but it has been shown that recurrent connections from learned outputs back to the reservoir can overcome these limits (Maass, Joshi, & Sontag, 2007). Thus, computational properties and limits of reservoir computing models continue to be investigated.

From the perspective of neuroscience, further work is needed to determine whether a homeostatic mechanism like the one proposed herein is operative in nervous systems. Findings of neuronal avalanches have been cited as prior evidence for critical branching in neural circuits (Beggs & Plenz, 2003; Petermann et al., 2009), although alternative explanations have been offered (Touboul & Destexhe, 2010). More recent analyses of LFP data argue against these alternatives (Friedman et al., 2012), and the present results bolster the case for critical branching in neural systems. Fractal spike trains and 1/f scaling now stand alongside neuronal avalanches as convergent evidence for critical branching.

This evidence does not shed light on neural processes that might give rise to critical branching, but the proposed tuning mechanism was essential for simulating the temporal scaling laws. This mechanism is different than most homeostatic tuning mechanisms hypothesized to operate on presynaptic inputs, rather than postsynaptic outputs (Turrigiano & Nelson, 2004). It is unclear whether presynaptic mechanisms could maintain critical branching or produce scaling laws, but there is evidence for postsynaptic tuning (Ibata, Sun, & Turrigiano, 2008). Thus, the currently formulated mechanism is at least consistent with the evidence.

Other neuroscience evidence, as well as behavioral evidence, indicates that intrinsic variations exhibit more than just scaling laws. A recent study showed that fluctuations in electrocorticographic activity not only exhibit scaling laws, but also the phase of fluctuations at lower frequencies has a modulatory effect on the amplitude of higher frequency fluctuations (He et al., 2010). This nesting of timescales is also consistent with findings of multifractal dynamics in spike trains (Baptista, Grebogi, & Köberle, 2006; Zheng, Gao, Sanchez, Principe, & Okun, 2005) as well as behavioral fluctuations (Ihlen & Vereijken, 2010; Stephen & Dixon, 2011). Multifractal dynamics have been associated with self-organized criticality (Turcotte, Malamud, Guzzetti, & Reichenbach, 2002), and multiplicative cascades that exhibit multifractal dynamics have been associated with branching processes (Q. Liu, 2000). Models like the one herein will need to address these and other findings that go beyond scaling laws, as evidence is gathered on conditions that yield multifractal fluctuations and other more complex phenomena.

Finally, let us end with the broadest perspectives from psychology and cognitive science. What does critical branching tell us about relations between neural and behavioral activity? Simon (1973) famously described hierarchical structures that appear universal to all natural and artificial systems of sufficient complexity. Cognitive systems are complex in this sense because, for example, neural and other physiological activities at lower levels hierarchically combine to form behaviors and functions at higher levels. Critical branching networks exhibited this kind of complexity, in that spikes formed spike patterns that were directly compared with network and behavioral activities.

However, the relation between hierarchical levels in critical branching models is importantly different from Simon's (1973) levels. Simon argued that levels are "nearly decomposable," meaning that interactions across components are weak relative to the stronger interactions holding each component together. While this is true to some extent, the property of metastability associated with criticality leads one to emphasize the "loosely composable" nature of cognitive systems as complex systems (see also Anderson, 2000). Synaptic connectivity composes neurons into networks, and critical branching allows spikes (fast timescale) to trigger changes in connectivity (slow timescale), which in turn change spike patterns, and so on between many slower and faster interacting timescales. These interactions result in multiscale dynamics that compose themselves into tenuously stable—metastable—shifting patterns (Hu et al., 2004; Usher et al., 1995). The balanced interplay between slower and faster timescales means that levels are less decomposable than suggested by Simon.

Metastability may be an appealing concept, but one must explain how specific perceptual and cognitive functions are formed and supported by metastable patterns. The reservoir computing analyses reported herein serve as preliminary work toward addressing this question, because they demonstrate one way that spike dynamics shaped by critical branching can be used for classification functions. Other studies have applied reservoir computing to a number of perceptual and cognitive functions, including speech recognition (Verstraeten, Schrauwen, Stroobandt, & Van Campenhout, 2005), syntactic processing (Tong, Bickett, Christiansen, & Cottrell, 2007), visual object motion tracking (Burgsteiner, Kröll, Leopold, & Steinbauer, 2007), motor control (Joshi & Maass, 2005), and navigation (Antonelo, Schrauwen, & Stroobandt, 2008). In fact, a precursor to the present model was applied to predicting directions and locations of various movement patterns (Szary & Kello, 2011).

An issue with all the above studies, and Simulation 2 herein, is that the readout functions were not used to classify metastable patterns per se. Metastability in the critical branching model is driven by engagement of the tuning mechanism, but the readout functions in Simulation 2 were applied to reservoir spikes *after* the mechanism was disengaged. Thus, connectivity was held constant for the readout function, so that relations between source inputs and reservoir spike patterns were held constant. By contrast, the tuning mechanism makes these relations dynamic, which requires a dynamic readout function in order to apply reservoir computing.

More generally, integrating learning mechanisms into critical branching neural networks would result in a spike-based, connectionist-like modeling framework (see also Aisa, Mingus, & O'Reilly, 2008). Critical branching models of cognitive functions would inherently explain scaling laws that are general and pervasive to cognitive performances. These models would also have inherent computational capacities on behaviorally relevant timescales, which would be generally useful for functions that unfold on the timescale of conscious performance and experience. Finally, the intrinsic variations produced near critical branching points may serve as a mechanism for sampling from generative models. It was mentioned at the outset that Boltzmann machines use stochastic variations to sample over probability distributions of features. The tuning mechanism herein was not designed to produce variations for sampling over distributions, although long-range memories of weakly chaotic network dynamics have been applied for this purpose (Welling & Chen, 2010), and a recent spiking network model was developed for this purpose (Buesing, Bill, Nessler, & Maass, 2011). It remains to be seen whether critical branching dynamics may be similarly applied.

References

Abraham, W. C. (2008). Metaplasticity: Tuning synapses and networks for plasticity. *Nature Reviews Neuroscience, 9, 387.* doi:10.1038/nrn2356

Ackley, D. H., Hinton, G. E., & Sejnowski, T. J. (1985). A learning algorithm for Boltzmann machines. *Cognitive Science, 9,* 147–169. doi:10.1207/s15516709cog0901_7

Aisa, B., Mingus, B., & O'Reilly, R. (2008). The Emergent neural modeling system. *Neural Networks, 21,* 1146–1152. doi:10.1016/j.neunet.2008.06.016

Anderson, C. M. (2000). From molecules to mindfulness: How vertically convergent fractal time fluctuations unify cognition and emotion. *Consciousness & Emotion, 1,* 193–226.

Antonelo, E. A., Schrauwen, B., & Stroobandt, D. (2008). Event detection and localization for small mobile robots using reservoir computing. *Neural Networks, 21,* 862–871. doi:10.1016/j.neunet.2008.06.010

Arieli, A., Sterkin, A., Grinvald, A., & Aertsen, A. (1996, September 27). Dynamics of ongoing activity: Explanation of the large variability in evoked cortical responses. *Science, 273,* 1868–1871. doi:10.1126/science.273.5283.1868

Baddeley, R., Abbott, L. F., Booth, M. C. A., Sengpiel, F., Freeman, T., Wakeman, E. A., & Rolls, E. T. (1997). Responses of neurons in primary and inferior temporal visual cortices to natural scenes. *Proceedings of the Royal Society B: Biological Sciences, 264,* 1775–1783. doi:10.1098/rspb.1997.0246

Bak, P., & Paczuski, M. (1995). Complexity, contingency, and criticality. *Proceedings of the National Academy of Sciences, USA, 92,* 6689–6696. doi:10.1073/pnas.92.15.6689

Bak, P., Tang, C., & Wiesenfeld, K. (1987). Self-organized criticality: An explanation of 1/f noise. *Physical Review Letters, 59,* 381–384. doi:10.1103/PhysRevLett.59.381

Baptista, M. S., Grebogi, C., & Köberle, R. (2006). Dynamically multilayered visual system of the multifractal fly. *Physical Review Letters, 97*(17), 178102. doi:10.1103/PhysRevLett.97.178102

Bédard, C., & Destexhe, A. (2009). Macroscopic models of local field potentials and the apparent 1/f noise in brain activity. *Biophysical Journal, 96,* 2589–2603. doi:10.1016/j.bpj.2008.12.3951

Beggs, J. M. (2008). The criticality hypothesis: How local cortical networks might optimize information processing. *Philosophical Transactions of the Royal Society A: Mathematical, Physical & Engineering Sciences, 366,* 329–343. doi:10.1098/rsta.2007.2092

Beggs, J. M., & Plenz, D. (2003). Neuronal avalanches in neocortical circuits. *The Journal of Neuroscience, 23,* 11167–11177.

Beltz, B. C., & Kello, C. T. (2006). On the intrinsic fluctuations of human behavior. In M. Vanchevsky (Ed.), *Focus on cognitive psychology research* (pp. 25–41). Hauppauge, NY: Nova Science.

Benayoun, M., Cowan, J. D., van Drongelen, W., & Wallace, E. (2010). Avalanches in a stochastic model of spiking neurons. *PLoS Computational Biology, 6*(7), e1000846. doi:10.1371/journal.pcbi.1000846

Bershadskii, A., Dremencov, E., Fukayama, D., & Yadid, G. (2001). Multifractal statistics and underlying kinetics of neuron spiking time-series. *Physics Letters A, 289,* 337–342. doi:10.1016/S0375-9601(01)00624-7

Bertschinger, N., & Natschlager, T. (2004). Real-time computation at the edge of chaos in recurrent neural networks. *Neural Computation, 16,* 1413–1436. doi:10.1162/089976604323057443

Bhattacharya, J., Edwards, J., Mamelak, A. N., & Schuman, E. M. (2005). Long-range temporal correlations in the spontaneous spiking of neurons in the hippocampal-amygdala complex of humans. *Neuroscience, 131,* 547–555. doi:10.1016/j.neuroscience.2004.11.013

Bressler, S. L., & Kelso, J. A. S. (2001). Cortical coordination dynamics and cognition. *Trends in Cognitive Sciences, 5,* 26–36. doi:10.1016/S1364-6613(00)01564-3

Brooks, V. B. (1986). *The neural basis of motor control*. New York, NY: Oxford University Press.

Brunel, N. (2000). Dynamics of sparsely connected networks of excitatory and inhibitory spiking neurons. *Journal of Computational Neuroscience, 8,* 183–208. doi:10.1023/A:1008925309027

Buesing, L., Bill, J., Nessler, B., & Maass, W. (2011). Neural dynamics as sampling: A model for stochastic computation in recurrent networks of spiking neurons. *PLoS Computational Biology, 7*(11), e1002211. doi:10.1371/journal.pcbi.1002211

Burgsteiner, H., Kröll, M., Leopold, A., & Steinbauer, G. (2007). Movement prediction from real-world images using a liquid state machine. *Applied Intelligence, 26,* 99–109. doi:10.1007/s10489-006-0007-1

Cao, J., & Wang, L. (2000). Periodic oscillatory solution of bidirectional associative memory networks with delays. *Physical Review E, 61,* 1825–1828. doi:10.1103/PhysRevE.61.1825

Carpenter, G. A., & Grossberg, S. G. (1987). A massively parallel architecture for a self-organizing neural pattern recognition machine. *Computer Vision, Graphics, and Image Processing, 37,* 54–115. doi:10.1016/S0734-189X(87)80014-2

Chklovskii, D. B., Schikorski, T., & Stevens, C. F. (2002). Wiring optimization in cortical circuits. *Neuron, 34,* 341–347. doi:10.1016/S0896-6273(02)00679-7

Cluff, T., & Balasubramaniam, R. (2009). Motor learning characterized by changing Lévy distributions. *PLoS ONE, 4*(6), e5998. doi:10.1371/journal.pone.0005998

Crutchfield, J. P., & Young, K. (1990). Computation at the edge of chaos. In W. Zurek (Ed.), *Entropy, complexity, and the physics of information* (pp. 223–269). Reading, MA: Addison-Wesley.

Dan, Y., & Poo, M.-m. (2004). Spike timing-dependent plasticity of neural circuits. *Neuron, 44,* 23–30. doi:10.1016/j.neuron.2004.09.007

Davidsen, J., & Paczuski, M. (2002). 1/f noise from correlations between avalanches in self-organized criticality. *Physical Review E, 66,* 050101(R). doi:10.1103/PhysRevE.66.050101

Davidsen, J., & Schuster, H. G. (2002). Simple model for $1/f^{\alpha}$ noise. *Physical Review E, 65*(2), 026120. doi:10.1103/PhysRevE.65.026120

de Arcangelis, L., & Herrmann, H. J. (2010). Learning as a phenomenon occurring in a critical state. *Proceedings of the National Academy of Sciences, USA, 107,* 3977–3981. doi:10.1073/pnas.0912289107

de Arcangelis, L., Perrone-Capano, C., & Herrmann, H. J. (2006). Self-organized criticality model for brain plasticity. *Physical Review Letters, 96*(2), 028107. doi:10.1103/PhysRevLett.96.028107

Ding, M., Chen, Y., & Kelso, J. (2002). Statistical analysis of timing errors. *Brain and Cognition, 48,* 98–106. doi:10.1006/brcg.2001.1306

Duarte, M., & Zatsiorsky, V. M. (2001). Long-range correlations in human standing. *Physics Letters A, 283*(1–2), 124–128. doi:10.1016/S0375-9601(01)00188-8

Elman, J. L. (1990). Finding structure in time. *Cognitive Science, 14,* 179–211. doi:10.1207/s15516709cog1402_1

Ermentrout, G. B. (2001, April 19). Oscillatory neural networks. Available from eLS–Wiley Online Library. doi:10.1038/npg.els.0000276

Farrell, S., Wagenmakers, E. J., & Ratcliff, R. (2006). 1/f noise in human cognition: Is it ubiquitous, and what does it mean? *Psychonomic Bulletin & Review, 13,* 737–741. doi:10.3758/BF03193989

Friedman, N., Ito, S., Brinkman, B. A. W., Shimono, M., DeVille, R. E. L., Dahmen, K. A., . . . Butler, T. C. (2012). Universal critical dynamics in high resolution neuronal avalanche data. *Physical Review Letters, 108*(20), 208102. doi:10.1103/PhysRevLett.108.208102

Friston, K. (2010). The free-energy principle: A unified brain theory? *Nature Reviews Neuroscience, 11,* 127–138. doi:10.1038/nrn2787

Ganguli, S., Huh, D., & Sompolinsky, H. (2008). Memory traces in dynamical systems. *Proceedings of the National Academy of Sciences, USA, 105,* 18970–18975. doi:10.1073/pnas.0804451105

Ganguli, S., & Sompolinsky, H. (2010). Statistical mechanics of compressed sensing. *Physical Review Letters, 104*(18), 188701. doi:10.1103/PhysRevLett.104.188701

Gerstein, G. L., & Mandelbrot, B. (1964). Random walk models for the spike activity of a single neuron. *Biophysical Journal, 4*(1), 41–68. doi:10.1016/S0006-3495(64)86768-0

Gilden, D. L. (2001). Cognitive emissions of 1/f noise. *Psychological Review, 108,* 33–56. doi:10.1037/0033-295X.108.1.33

Gilden, D. L. (2009). Global model analysis of cognitive variability. *Cognitive Science, 33,* 1441–1467. doi:10.1111/j.1551-6709.2009.01060.x

Gilden, D. L., & Hancock, H. (2007). Response variability in attention-deficit disorders. *Psychological Science, 18,* 796–802. doi:10.1111/j.1467-9280.2007.01982.x

Gilden, D. L., Thornton, T., & Mallon, M. W. (1995, March 24). 1/f noise in human cognition. *Science, 267,* 1837–1839. doi:10.1126/science.7892611

Granger, C. W. J. (1980). Long memory relationships and the aggregation of dynamic models. *Journal of Econometrics, 14,* 227–238. doi:10.1016/0304-4076(80)90092-5

Granger, C. W. J., & Joyeux, R. (1980). An introduction to long-memory models and fractional differencing. *Journal of Time Series Analysis, 1,* 15–29. doi:10.1111/j.1467-9892.1980.tb00297.x

Hahn, G., Petermann, T., Havenith, M. N., Yu, S., Singer, W., Plenz, D., & Nikolić, D. (2010). Neuronal avalanches in spontaneous activity in vivo. *Journal of Neurophysiology, 104,* 3312–3322. doi:10.1152/jn.00953.2009

Haldeman, C., & Beggs, J. M. (2005). Critical branching captures activity in living neural networks and maximizes the number of metastable states. *Physical Review Letters, 94*(5), 058101. doi:10.1103/PhysRevLett.94.058101

Harm, M. W., & Seidenberg, M. S. (1999). Phonology, reading acquisition, and dyslexia: Insights from connectionist models. *Psychological Review, 106,* 491–528. doi:10.1037/0033-295X.106.3.491

Harris, T. E. (1989). *The theory of branching processes*. New York, NY: Dover.

Hayer, A., & Bhalla, U. S. (2005). Molecular switches at the synapse emerge from receptor and kinase traffic. *PLoS Computational Biology, 1*(2), e20. doi:10.1371/journal.pcbi.0010020

He, B. J., Zempel, J. M., Snyder, A. Z., & Raichle, M. E. (2010). The temporal structures and functional significance of scale-free brain activity. *Neuron, 66,* 353–369. doi:10.1016/j.neuron.2010.04.020

Higley, M. J., & Contreras, D. (2006). Balanced excitation and inhibition determine spike timing during frequency adaptation. *The Journal of Neuroscience, 26,* 448–457. doi:10.1523/JNEUROSCI.3506-05.2006

Hinton, G. E. (1989). Connectionist learning procedures. *Artificial Intelligence, 40*(1–3), 185–234. doi:10.1016/0004-3702(89)90049-0

Hinton, G. E., Osindero, S., & Teh, Y.-W. (2006). A fast learning algorithm for deep belief nets. *Neural Computation, 18,* 1527–1554. doi:10.1162/neco.2006.18.7.1527

Hobbs, J. P., Smith, J. L., & Beggs, J. M. (2010). Aberrant neuronal avalanches in cortical tissue removed from juvenile epilepsy patients. *Journal of Clinical Neurophysiology, 27,* 380–386.

Holden, J. G., Choi, I., Amazeen, P. G., & Van Orden, G. (2011). Fractal 1/f dynamics suggest entanglement of measurement and human performance. *Journal of Experimental Psychology: Human Perception and Performance, 37,* 935–948. doi:10.1037/a0020991

Holden, J. G., Van Orden, G. C., & Turvey, M. T. (2009). Dispersion of response times reveals cognitive dynamics. *Psychological Review, 116,* 318–342. doi:10.1037/a0014849

Holmgren, C. D., & Zilberter, Y. (2001). Coincident spiking activity induces long-term changes in inhibition of neocortical pyramidal cells. *The Journal of Neuroscience, 21,* 8270–8277.

Hopfield, J. J. (1982). Neural networks and physical systems with emergent collective computational abilities. *Proceedings of the National Academy of Sciences, USA, 79,* 2554–2558. doi:10.1073/pnas.79.8.2554

Hotton, S., & Yoshimi, J. (2011). Extending dynamical systems theory to model embodied cognition. *Cognitive Science, 35,* 444–479. doi:10.1111/j.1551-6709.2010.01151.x

Hsu, D., & Beggs, J. M. (2006). Neuronal avalanches and criticality: A dynamical model for homeostasis. *Neurocomputing, 69,* 1134–1136. doi:10.1016/j.neucom.2005.12.060

Hu, K., Ivanov, P. C., Chen, Z., Hilton, M. F., Stanley, H. E., & Shea, S. A. (2004). Non-random fluctuations and multi-scale dynamics regulation of human activity. *Physica A: Statistical Mechanics and its Applications, 337*(1–2), 307–318.

Ibata, K., Sun, Q., & Turrigiano, G. G. (2008). Rapid synaptic scaling induced by changes in postsynaptic firing. *Neuron, 57,* 819–826. doi:10.1016/j.neuron.2008.02.031

Ihlen, E. A., & Vereijken, B. (2010). Interaction-dominant dynamics in human cognition: Beyond 1/fα fluctuation. *Journal of Experimental Psychology: General, 139,* 436–463. doi:10.1037/a0019098

Iyengar, S., & Liao, Q. (1997). Modeling neural activity using the generalized inverse Gaussian distribution. *Biological Cybernetics, 77,* 289–295. doi:10.1007/s004220050390

Jackson, B. S. (2004). Including long-range dependence in integrate-and-fire models of the high interspike-interval variability of cortical neurons. *Neural Computation, 16,* 2125–2195. doi:10.1162/0899766041732413

Jaeger, H., Maass, W., & Principe, J. (2007). Editorial: Special issue on echo state networks and liquid state machines. *Neural Networks, 20,* 287–289. doi:10.1016/j.neunet.2007.04.001

Jensen, H. J. (1998). *Self-organized criticality*. Cambridge, England: Cambridge University Press.

Joshi, P., & Maass, W. (2005). Movement generation with circuits of spiking neurons. *Neural Computation, 17,* 1715–1738. doi:10.1162/0899766054026684

Katchalsky, A., & Kedemo, O. (1962). Thermodynamics of flow processes in biological systems. *Biophysical Journal, 2*(2), 53–78. doi:10.1016/S0006-3495(62)86948-3

Kello, C. (2011). Intrinsic fluctuations yield pervasive 1/f scaling: Comment on Moscoso del Prado Martín (2011). *Cognitive Science, 35,* 838–841. doi:10.1111/j.1551-6709.2011.01185.x

Kello, C. T., Anderson, G. G., Holden, J. G., & Van Orden, G. C. (2008). The pervasiveness of 1/f scaling in speech reflects the metastable basis of cognition. *Cognitive Science, 32,* 1217–1231. doi:10.1080/03640210801944898

Kello, C. T., Beltz, B. C., Holden, J. G., & Van Orden, G. C. (2007). The emergent coordination of cognitive function. *Journal of Experimental Psychology: General, 136,* 551–568. doi:10.1037/0096-3445.136.4.551

Kello, C. T., Brown, G. D. A., Ferrer-i-Cancho, R., Holden, J. G., Linkenkaer-Hansen, K., Rhodes, T., & Van Orden, G. C. (2010). Scaling laws in cognitive sciences. *Trends in Cognitive Sciences, 14,* 223–232. doi:10.1016/j.tics.2010.02.005

Kello, C. T., & Kawamoto, A. H. (1998). Runword: An IBM-PC software package for the collection and acoustic analysis of speeded naming responses. *Behavior Research Methods, Instruments, & Computers, 30,* 371–383. doi:10.3758/BF03200668

Kello, C., & Kerster, B. (2011, April 11). Power laws, memory capacity, and self-tuned critical branching in an LIF model with binary synapses. In *Proceedings of Computational and Systems Neuroscience 2011*. Available from Nature Precedings. doi:10.1038/npre.2011.5893.1

Kello, C. T., Kerster, B., & Johnson, E. (2011). Critical branching neural computation, neural avalanches, and 1/f scaling. In L. Carlson, C. Hoelscher, & T. F. Shipley (Eds.), *Proceedings of the 33rd Annual Meeting of the Cognitive Science Society* (pp. 1685–1690). Boston, MA: Cognitive Science Society.

Kello, C. T., & Mayberry, M. R. (2010). Critical branching neural computation. In *International Joint Conference on Neural Networks* (pp. 1475–1481). Barcelona, Spain: IEEE.

Kello, C. T., & Van Orden, G. C. (2009). Soft-assembly of sensorimotor function. *Nonlinear Dynamics, Psychology, and Life Sciences, 13,* 57–78.

Kelso, J. A. S. (1995). *Dynamic patterns: The self-organization of brain and behavior*. Cambridge, MA: MIT Press.

Kinouchi, O., & Copelli, M. (2006). Optimal dynamical range of excitable networks at criticality. *Nature Physics, 2,* 348–351. doi:10.1038/nphys289

Kwok, T., & Smith, K. A. (2005). Optimization via intermittency with a self-organizing neural network. *Neural Computation, 17,* 2454–2481. doi:10.1162/0899766054796860

Langton, C. G. (1990). Computation at the edge of chaos: Phase transitions and emergent computation. *Physica D: Nonlinear Phenomena, 42*(1–3), 12–37. doi:10.1016/0167-2789(90)90064-V

Large, E. W., & Kolen, J. F. (1994). Resonance and the perception of musical meter. *Connection Science, 6,* 177–208. doi:10.1080/09540099408915723

Laufs, H., Krakow, K., Sterzer, P., Eger, E., Beyerle, A., Salek-Haddadi, A., & Kleinschmidt, A. (2003). Electroencephalographic signatures of attentional and cognitive default modes in spontaneous brain activity fluctuations at rest. *Proceedings of the National Academy of Sciences, USA, 100,* 11053–11058. doi:10.1073/pnas.1831638100

Linkenkaer-Hansen, K., Monto, S., Rytsala, H., Suominen, K., Isometsa, E., & Kahkonen, S. (2005). Breakdown of long-range temporal correlations in theta oscillations in patients with major depressive disorder. *The Journal of Neuroscience, 25,* 10131–10137. doi:10.1523/JNEUROSCI.3244-05.2005

Linkenkaer-Hansen, K., Nikouline, V. V., Palva, J. M., & Ilmoniemi, R. J. (2001). Long-range temporal correlations and scaling behavior in human brain oscillations. *The Journal of Neuroscience, 21,* 1370–1377.

Linkenkaer-Hansen, K., Nikulin, V. V., Palva, J. M., Kaila, K., & Ilmoniemi, R. J. (2004). Stimulus-induced change in long-range temporal correlations and scaling behaviour of sensorimotor oscillations. *European Journal of Neuroscience, 19,* 203–218. doi:10.1111/j.1460-9568.2004.03116.x

Lisman, J. E., & McIntyre, C. C. (2001). Synaptic plasticity: A molecular memory switch. *Current Biology, 11,* R788–R791. doi:10.1016/S0960-9822(01)00472-9

Liu, Q. (2000). On generalized multiplicative cascades. *Stochastic Processes and Their Applications, 86,* 263–286. doi:10.1016/S0304-4149(99)00097-6

Liu, Z., Fukunaga, M., de Zwart, J. A., & Duyn, J. H. (2010). Large-scale spontaneous fluctuations and correlations in brain electrical activity observed with magnetoencephalography. *NeuroImage, 51,* 102–111. doi:10.1016/j.neuroimage.2010.01.092

Lübeck, S. (2004). Universal scaling behavior of non-equilibrium phase transitions. *International Journal of Modern Physics B, 18*(31, No. 32), 3977. doi:10.1142/S0217979204027748

Maass, W. (1997). Networks of spiking neurons: The third generation of neural network models. *Neural Networks, 10,* 1659–1671. doi:10.1016/S0893-6080(97)00011-7

Maass, W., Joshi, P., & Sontag, E. D. (2007). Computational aspects of feedback in neural circuits. *PLoS Computational Biology, 3*(1), e165. doi:10.1371/journal.pcbi.0020165

Maass, W., Natschlager, T., & Markram, H. (2002). Real-time computing without stable states: A new framework for neural computation based on perturbations. *Neural Computation, 14,* 2531–2560. doi:10.1162/089976602760407955

Marder, E., & Goaillard, J.-M. (2006). Variability, compensation and homeostasis in neuron and network function. *Nature Reviews Neuroscience, 7,* 563–574. doi:10.1038/nrn1949

Markram, H., Lübke, J., Frotscher, M., & Sakmann, B. (1997, January 10). Regulation of synaptic efficacy by coincidence of postsynaptic APs and EPSPs. *Science, 275,* 213–215. doi:10.1126/science.275.5297.213

Marr, D. (1982). *Vision: A computational investigation into the human representation and processing of visual information*. San Francisco, CA: Freeman.

Mattia, M., & Del Giudice, P. (2000). Efficient event-driven simulation of large networks of spiking neurons and dynamical synapses. *Neural Computation, 12,* 2305–2329. doi:10.1162/089976600300014953

Mazzoni, A., Broccard, F. D., Garcia-Perez, E., Bonifazi, P., Ruaro, M. E., & Torre, V. (2007). On the dynamics of the spontaneous activity in neuronal networks. *PLoS ONE, 2*(5), e439. doi:10.1371/journal.pone.0000439

McClung, C. A., Ulery, P. G., Perrotti, L. I., Zachariou, V., Berton, O., & Nestler, E. J. (2004). ΔFosB: A molecular switch for long-term adaptation in the brain. *Molecular Brain Research, 132,* 146–154. doi:10.1016/j.molbrainres.2004.05.014

Micheva, K. D., Busse, B., Weiler, N. C., O'Rourke, N., & Smith, S. J. (2010). Single-synapse analysis of a diverse synapse population: Proteomic imaging methods and markers. *Neuron, 68,* 639–653. doi:10.1016/j.neuron.2010.09.024

Mitchell, M., Hraber, P. T., & Crutchfield, J. P. (1999). Dynamic computation, and the "edge of chaos": A re-examination. In G. Cowan, D. Pines, & D. Melzner (Eds.), *Complexity: Metaphors, models, and reality* (pp. 497–513). Reading, MA: Addison-Wesley.

Montez, T., Poil, S.-S., Jones, B. F., Manshanden, I., Verbunt, J. P. A., van Dijk, B. W., . . . Linkenkaer-Hansen, K. (2009). Altered temporal correlations in parietal alpha and prefrontal theta oscillations in early-stage Alzheimer disease. *Proceedings of the National Academy of Sciences, USA, 106,* 1614–1619. doi:10.1073/pnas.0811699106

Moscoso del Prado Martín, F. (2011). Causality, criticality, and reading words: Distinct sources of fractal scaling in behavioral sequences. *Cognitive Science, 35,* 785–837. doi:10.1111/j.1551-6709.2011.01184.x

O'Connor, D. H., Wittenberg, G. M., & Wang, S. S.-H. (2005). Graded bidirectional synaptic plasticity is composed of switch-like unitary events. *Proceedings of the National Academy of Sciences, USA, 102,* 9679–9684. doi:10.1073/pnas.0502332102

Packard, N. (1988). Adaptation towards the edge of chaos. In J. A. S. Kelso, A. J. Mandell, & M. F. Shlesinger (Eds.), *Dynamic patterns in complex systems* (pp. 293–301). Singapore: World Scientific.

Pearlmutter, B. A. (1995). Gradient calculations for dynamic recurrent neural networks: A survey. *IEEE Transactions on Neural Networks, 6,* 1212–1228. doi:10.1109/72.410363

Petermann, T., Thiagarajan, T. C., Lebedev, M. A., Nicolelis, M. A. L., Chialvo, D. R., & Plenz, D. (2009). Spontaneous cortical activity in awake monkeys composed of neuronal avalanches. *Proceedings of the National Academy of Sciences, USA, 106,* 15921–15926. doi:10.1073/pnas.0904089106

Petersen, C. C. H., Malenka, R. C., Nicoll, R. A., & Hopfield, J. J. (1998). All-or-none potentiation at CA3-CA1 synapses. *Proceedings of the National Academy of Sciences, USA, 95,* 4732–4737. doi:10.1073/pnas.95.8.4732

Poil, S.-S., van Ooyen, A., & Linkenkaer-Hansen, K. (2008). Avalanche dynamics of human brain oscillations: Relation to critical branching processes and temporal correlations. *Human Brain Mapping, 29,* 770–777. doi:10.1002/hbm.20590

Rabinovich, M. I., Huerta, R., Varona, P., & Afraimovich, V. S. (2008). Transient cognitive dynamics, metastability, and decision making. *PLoS Computational Biology, 4*(5), e1000072. doi:10.1371/journal.pcbi.1000072

Raichle, M. E., & Gusnard, D. A. (2005). Intrinsic brain activity sets the stage for expression of motivated behavior. *The Journal of Comparative Neurology, 493,* 167–176. doi:10.1002/cne.20752

Raichle, M. E., MacLeod, A. M., Snyder, A. Z., Powers, W. J., Gusnard, D. A., & Shulman, G. L. (2001). A default mode of brain function. *Proceedings of the National Academy of Sciences, USA, 98,* 676–682. doi:10.1073/pnas.98.2.676

Rangarajan, G., & Ding, M. (2000). Integrated approach to the assessment of long range correlation in time series data. *Physical Review E, 61,* 4991–5001. doi:10.1103/PhysRevE.61.4991

Rasouli, G., Rasouli, M., Lenz, F. A., Verhagen, L., Borrett, D. S., & Kwan, H. C. (2006). Fractal characteristics of human Parkinsonian neuronal spike trains. *Neuroscience, 139,* 1153–1158. doi:10.1016/j.neuroscience.2006.01.012

Rieke, F., Warland, D., van Steveninck, R. d. R., & Bialek, W. (1996). *Spikes: Exploring the neural code*. Cambridge, MA: MIT Press.

Riley, M. A., & Turvey, M. (2002). Variability and determinism in motor behavior. *Journal of Motor Behavior, 34,* 99–125. doi:10.1080/00222890209601934

Robin, K., Maurice, N., Degos, B., Deniau, J.-M., Martinerie, J., & Pezard, L. (2009). Assessment of bursting activity and interspike intervals variability: A case study for methodological comparison. *Journal of Neuroscience Methods, 179,* 142–149. doi:10.1016/j.jneumeth.2009.01.020

Rowat, P. (2007). Interspike interval statistics in the stochastic Hodgkin–Huxley model: Coexistence of gamma frequency bursts and highly irregular firing. *Neural Computation, 19,* 1215–1250. doi:10.1162/neco.2007.19.5.1215

Rumelhart, D. E., Hinton, G. E., & Williams, R. J. (1986, October 9). Learning representations by back-propagating errors. *Nature, 323,* 533–536. doi:10.1038/323533a0

Shadlen, M. N., & Newsome, W. T. (1998). The variable discharge of cortical neurons: Implications for connectivity, computation, and information coding. *The Journal of Neuroscience, 18,* 3870–3896.

Shew, W. L., Yang, H., Petermann, T., Roy, R., & Plenz, D. (2009). Neuronal avalanches imply maximum dynamic range in cortical networks at criticality. *The Journal of Neuroscience, 29,* 15595–15600. doi:10.1523/JNEUROSCI.3864-09.2009

Shin, C. W., & Kim, S. (2006). Self-organized criticality and scale-free properties in emergent functional neural networks. *Physical Review E, 74*(4), 045101. doi:10.1103/PhysRevE.74.045101

Shockley, K., Santana, M. V., & Fowler, C. A. (2003). Mutual interpersonal postural constraints are involved in cooperative conversation. *Journal of Experimental Psychology: Human Perception and Performance, 29,* 326–332. doi:10.1037/0096-1523.29.2.326

Shu, Y., Hasenstaub, A., & McCormick, D. A. (2003, May 15). Turning on and off recurrent balanced cortical activity. *Nature, 423,* 288–293. doi:10.1038/nature01616

Simon, H. A. (1973). The organization of complex systems. In H. H. Pattee (Ed.), *Hierarchy theory: The challenge of complex systems* (pp. 1–27). New York, NY: George Braziller.

Smith, P. L., & Ratcliff, R. (2004). Psychology and neurobiology of simple decisions. *Trends in Neurosciences, 27,* 161–168. doi:10.1016/j.tins.2004.01.006

Softky, W. R., & Koch, C. (1993). The highly irregular firing of cortical cells is inconsistent with temporal integration of random EPSPs. *The Journal of Neuroscience, 13,* 334–350.

Song, S., Miller, K. D., & Abbott, L. F. (2000). Competitive Hebbian learning through spike-timing-dependent synaptic plasticity. *Nature Neuroscience, 3,* 919–926. doi:10.1038/78829

Sornette, D. (2004). *Critical phenomena in natural sciences: Chaos, fractals, self-organization, and disorder: Concepts and tools* (2nd ed.). New York, NY: Springer.

Spivey, M. J. (2007). *The continuity of mind*. New York, NY: Oxford University Press.

Stanley, H. E. (1987). *Introduction to phase transitions and critical phenomena*. New York, NY: Oxford University Press.

Stein, R. B., Gossen, E. R., & Jones, K. E. (2005). Neuronal variability: Noise or part of the signal? *Nature Reviews Neuroscience, 6,* 389–397. doi:10.1038/nrn1668

Stellwagen, D., & Malenka, R. C. (2006, April 20). Synaptic scaling mediated by glial TNF-α. *Nature, 440,* 1054–1059. doi:10.1038/nature04671

Stephen, D. G., & Dixon, J. A. (2011). Strong anticipation: Multifractal cascade dynamics modulate scaling in synchronization behaviors. *Chaos, Solitons & Fractals, 44*(1–3), 160–168. doi:10.1016/j.chaos.2011.01.005

Swenson, R., & Turvey, M. (1991). Thermodynamic reasons for perception–action cycles. *Ecological Psychology, 3,* 317–348. doi:10.1207/s15326969eco0304_2

Szary, J., & Kello, C. T. (2011). *Visual motion perception using critical branching neural computation*. Paper presented at the 34th Annual Meeting of the Cognitive Science Society, Boston, MA.

Teich, M. C., Heneghan, C., Lowen, S. B., Ozaki, T., & Kaplan, E. (1997). Fractal character of the neural spike train in the visual system of the cat. *Journal of the Optical Society of America A, 14,* 529–546. doi:10.1364/JOSAA.14.000529

Teich, M. C., & Lowen, S. B. (1994, April–May). Fractal patterns in auditory nerve-spike trains. *Engineering in Medicine and Biology Magazine, IEEE, 13*(2), 197–202. doi:10.1109/51.281678

Thornton, T. L., & Gilden, D. L. (2005). Provenance of correlations in psychological data. *Psychonomic Bulletin & Review, 12,* 409–441. doi:10.3758/BF03193785

Tong, M. H., Bickett, A. D., Christiansen, E. M., & Cottrell, G. W. (2007). Learning grammatical structure with Echo State Networks. *Neural Networks, 20,* 424–432. doi:10.1016/j.neunet.2007.04.013

Torre, K., & Wagenmakers, E.-J. (2009). Theories and models for $1/f^{\beta}$ noise in human movement science. *Human Movement Science, 28,* 297–318. doi:10.1016/j.humov.2009.01.001

Touboul, J., & Destexhe, A. (2010). Can power-law scaling and neuronal avalanches arise from stochastic dynamics? *PLoS ONE, 5(2),* e8982. doi:10.1371/journal.pone.0008982

Troyer, T. W., & Miller, K. D. (1997). Physiological gain leads to high ISI variability in a simple model of a cortical regular spiking cell. *Neural Computation, 9,* 971–983. doi:10.1162/neco.1997.9.5.971

Turcotte, D. L., Malamud, B. D., Guzzetti, F., & Reichenbach, P. (2002). Self-organization, the cascade model, and natural hazards. *Proceedings of the National Academy of Sciences, USA, 99*(Suppl. 1), 2530–2537. doi:10.1073/pnas.012582199

Turrigiano, G. G., & Nelson, S. B. (2004). Homeostatic plasticity in the developing nervous system. *Nature Reviews Neuroscience, 5,* 97–107. doi:10.1038/nrn1327

Usher, M., Stemmler, M., Koch, C., & Olami, Z. (1994). Network amplification of local fluctuations causes high spike rate variability, fractal firing patterns and oscillatory local field potentials. *Neural Computation, 6,* 795–836. doi:10.1162/neco.1994.6.5.795

Usher, M., Stemmler, M., & Olami, Z. (1995). Dynamic pattern-formation leads to 1/f noise in neural populations. *Physical Review Letters, 74,* 326–329. doi:10.1103/PhysRevLett.74.326

Van Orden, G. C., Holden, J. G., & Turvey, M. T. (2003). Self-organization of cognitive performance. *Journal of Experimental Psychology: General, 132,* 331–350. doi:10.1037/0096-3445.132.3.331

Van Orden, G. C., Kello, C. T., & Holden, J. G. (2010). Situated behavior and the place of measurement in psychological theory. *Ecological Psychology, 22,* 24–43. doi:10.1080/10407410903493145

van Vreeswijk, C., & Sompolinsky, H. (1996, December 6). Chaos in neuronal networks with balanced excitatory and inhibitory activity. *Science, 274,* 1724–1726. doi:10.1126/science.274.5293.1724

Verstraeten, D., Schrauwen, B., Stroobandt, D., & Van Campenhout, J. (2005). Isolated word recognition with the Liquid State Machine: A case study. *Information Processing Letters, 95,* 521–528. doi:10.1016/j.ipl.2005.05.019

Wagenmakers, E.-J., Farrell, S., & Ratcliff, R. (2004). Estimation and interpretation of l/f alpha noise in human cognition. *Psychonomic Bulletin & Review, 11,* 579–615. doi:10.3758/BF03196615

Welling, M., & Chen, Y. (2010). Statistical inference using weak chaos and infinite memory. *Journal of Physics: Conference Series,* 233(1), 012005. doi:10.1088/1742-6596/233/1/012005

Wolpert, D. H., & Macready, W. G. (1997). No free lunch theorems for optimization. *IEEE Transactions on Evolutionary Computation, 1,* 67–82.

Zapperi, S., Lauritsen, K. B., & Stanley, H. E. (1995). Self-organized branching processes: Mean-field theory for avalanches. *Physical Review Letters, 75,* 4071–4074. doi:10.1103/PhysRevLett.75.4071

Zheng, Y., Gao, J., Sanchez, J. C., Principe, J. C., & Okun, M. S. (2005). Multiplicative multifractal modeling and discrimination of human neuronal activity. *Physics Letters A, 344*(2–4), 253–264. doi:10.1016/j.physleta.2005.06.092

Received November 22, 2011
Revision received August 29, 2012
Accepted October 19, 2012 ■